

Geochemical evaluation of cosmic spherules collected from the Central Indian Ocean Basin.

M. Pandey^{1, 2*}, N.G. Rudraswami^{1*}, V. P. Singh^{1, 3} and A. Viegas²

¹National Institute of Oceanography (Council of Scientific and Industrial Research),
Dona Paula, Goa 403004, India

²School of Earth, Ocean and Atmospheric Sciences, Goa University
Goa 403206, India

³Academy of Scientific and Innovative Research (AcSIR),
Ghaziabad 201002, India

*Corresponding Author: rudra@nio.org

Abstract

Micrometeorites (MMs) significantly contribute to the extraterrestrial material the Earth receives and represent a broader range of precursors than known meteorites. Low sedimentation rates prevalent in the deep-sea regions far away from land provide a unique opportunity for collecting MMs from these least disturbed regions. In the present study, we have studied 305 cosmic spherules recovered from the Central Indian Ocean Basin (CIOB); that have undergone melting during hypervelocity entry into the Earth's atmosphere. During the atmospheric entry, primary signatures of MMs are lost depending upon the extent of heating, complicating the identification of the parent body. Nevertheless, we have tried to relate these cosmic spherules to their respective parent bodies based on elemental ratios present in them, considering atmospheric ablative losses of various elements. The chemical analyses indicate that many deep-sea cosmic spherules are linked to carbonaceous chondrites. Around 239 porphyritic olivines (PO), 42 relict olivines are studied for their textural development and composition during recrystallisation during atmospheric entry. Thirty-zoned olivines are analysed from rim to core to understand various elements' behaviour during atmospheric entry. Seawater plays a vital role in eroding these cosmic spherules' material, and its effect is also discussed. As most of the recent micrometeorite collections focus on the polar region, these deep-sea spherules will significantly add to the information about the extraterrestrial matter reaching the Earth.

Keywords : Micrometeorites; Cosmic Spherule; Chondrite; Atmospheric entry.

1. Introduction

Micrometeorites (MMs) have been the most dominant extraterrestrial material accreted by the Earth's surface, with sizes ranging from 10's of μm to a few mm (Rubin & Grossman, 2010), generated by either asteroidal collisions or sublimation of cometary bodies (Kurat et al., 1994; Genge et al., 1997; Genge et al., 2008; Plane, 2012; Noguchi et al., 2015), followed by their transportation governed by non-gravitational forces such as Poynting-Robertson Drag (Bottke et al., 2006). The MMs endure frictional heating leading to melting of various degrees depending upon entry velocity, entry angle and particle size (Taylor et al., 1998; Genge et al., 2008; Rudraswami et al., 2015). Cosmic spherules provide relatively less biased samples of extraterrestrial material than conventional meteorites (Brownlee et al., 1997), thereby providing an exceptional opportunity to infer diverse solar system processes and their objects. MMs experience frictional heating during atmospheric entry, which can alter the chemical, isotopic and textural features depending upon various entry factors such as entry angle, entry velocity, particle size, parent body and chemical composition. A comprehensive account of atmospheric entry and changes that occurred can be found in various literature (Flynn, 1989; Love and Brownlee, 1991; Toppani et al., 2001; Briani et al., 2013; Rudraswami et al., 2016). Melted MMs have undergone a variable degree of melting, recrystallisation and thermal alterations and provide clues of processes occurring during atmospheric entry. In contrast, unmelted ones preserve their primitive nature, experiencing minimal alteration. Their original chemistry remains largely preserved, making it possible to identify the particle's pre-entry mineralogy that provides a direct window for the study of nature and origins of their parent body. MMs are ubiquitous and fall at the rate of around 40,000 tons per annum on the top of the Earth's atmosphere, estimated using the Long Duration Exposure Facility satellite with an altitude of $\sim 331\text{--}480$ km (Love and Brownlee, 1993). The flux of MMs has always remained a contentious issue. Various workers have attempted to estimate flux in different environments and time scales using a variety of methods such as measuring hypervelocity craters on the thermal control panel of the Long Duration Exposure Facility (Love and Brownlee, 1993), concentrations of ^3He in deep-sea sediments (Parkin and Tilles, 1968; Takayanagi and Ozima, 1987), Os and Ir concentrations in the deep-sea sediments (Peucker-Ehrenbrink and Ravizza, 2000), handpicked MMs (Yada et al., 2004; Prasad et al., 2013). The cosmic spherules collection is done in areas with minimal terrestrial input or anthropogenic contamination. They were first recovered in the late nineteenth century during the famous voyage of HMS Challenger from the deep sea floor of the Pacific Ocean (Murray and Renard, 1891). After that, they are recovered from various environments by numerous workers, mainly from the deep sea (Bruun et al., 1955; Finkelman et al., 1970;

Blanchard et al., 1980; Brownlee, 1984; Prasad et al., 2013; Swain, 2021), Antarctic ice (Maurette et al., 1991; Taylor et al., 1998; Goderis et al., 2020; Rudraswami et al., 2018a, 2021), Antarctic snow (Taylor et al., 1998, 2000; Nakamura et al., 1999; Duprat et al., 2007), and bare-rock traps in Antarctica (Rochette et al., 2008; Suavet et al., 2009) varved lake sediments (Akulov et al., 2014), fluvial deposits (Bi et al., 1993), cryoconite lakes in Greenland (Maurette et al., 1987), Beach Sand (Marvin and Einaudi, 1967), and urban areas (Genge et al., 2017; Suttle et al., 2021). One of the most critical aspects of studying cosmic spherules is to link their precursors, thereby understanding the nature of dust-producing solar system bodies reaching the Earth's surface. Previous studies have shown that most MMs represent samples from chondritic parent bodies largely dominated by carbonaceous chondrites. However, the opinion regarding the dominance of carbonaceous chondrites over ordinary ones is still evolving (Prasad et al., 2015; Genge et al., 2008; Suavet et al., 2010; Van Ginneken et al., 2012). Very few examples of MMs belong to the achondrites (Cordier et al., 2011; Taylor et al., 2007; Gounelle et al., 2009; Soens et al., 2022). In this study, we have analysed the bulk chemical composition of cosmic spherules and have classified them into various textural classes. We have identified their parent bodies based on the bulk chemical composition, elemental ratios, and minor oxides of relict olivines. The changes observed in their texture and composition during atmospheric entry are documented, particularly olivines formed by the recrystallisation of partial melt. The interaction of seawater and cosmic spherules due to etching is an essential phenomenon in contributing to the primary productivity in oceans (Rudraswami et al., 2021); the effect of ocean water on cosmic spherules based on the geochemical data is discussed.

2. Materials and Methods

We have analysed 305 cosmic spherules recovered from sediments of the Central Indian Ocean Basin (CIOB). These sediments were collected using Okean grab at a water depth of more than ~5000 m during Polymetallic Nodule Survey cruise SSD 48 conducted by CSIR- National Institute of Oceanography (CSIR-NIO) from 31-03-2018 to 05-05-2018. The samples utilized for this study have been taken from two stations (13° 44.9949', 74° 48.7655' and 13° 44.9961', 74° 56.2669') and the location map is given in Fig.1. The total wet-sieved sediments weigh ~1.4 tons and its equivalent weight of subsequent dried sample is ~ 355 kg. Out of 1.4 tons of wet sieved sediment around 70 kg of wet-sieved sediment having equivalent dry weight of ~18 kg is utilised to recover cosmic spherules for this study. The wet sediments were sieved using a sieve size of ~220 µm. The dried sediment fraction was subjected to magnetic separation using the hand-held magnet, and the separated fraction was scanned under a stereoscopic microscope for hand-picking probable cosmic spherules, which are spherical in morphology. All the handpicked spherules were mounted on epoxy.

The mounts were ground and polished, followed by ultrasonic cleaning using alcohol and distilled water. The cleaned and dried mounts were coated with carbon to make surface conduct for analyses using electron microscopy. High-quality back-scattered electron (BSE) images at different magnifications are obtained using a scanning electron microscope (SEM, JEOL JSM IT 300). Further quantitative elemental analysis is acquired using electron microprobe (Cameca SX Five) at the National Institute of Oceanography (NIO), Goa. The beam current used for analysis is 12nA at 15 kV. The beam diameter is set to be 1–2 μ m. Multiple spots were analysed on each spherule for better precision and averaged to determine their bulk chemical composition.

3. Results

3.1 Description and types of MMs

The total number of spherules recovered in this study was 305; however, only 267 cosmic spherules are reported here as due to harsh conditions prevalent in the ocean, many spherules undergo extreme etching during their residence time in seawater followed by their burial in sediments and have very poor preservation posing difficulty in picking, mounting and analysing the sample for their chemical composition. The diameter of spherules in the present study ranges from 140–450 μ m (Fig. 2) and is largely dominated by the spherules having a diameter in the range of ~200 μ m. The spherules here can be broadly divided into barred, porphyritic, glass, relict grain bearing (RGB), Iron, and G-type based on textural parameters. Representative BSE images of these spherules are shown in (Fig. 3). The barred cosmic spherules dominates other, followed by porphyritic type and I-type. Cryptocrystalline and RGB are similar in quantity (Fig. 4). Glass cosmic spherules are less as compared to cryptocrystalline (Fig. 4). There are only three scoriaceous cosmic spherules. The relative number and types of cosmic spherules are given in (Fig. 4). The details of the spherule types are provided in the subsequent section.

3.1.1 Porphyritic and Relict grain bearing (RGB)

The porphyritic olivine spherules are dominated by phenocrysts of olivine, along with glassy mesostasis. They comprise ~18% of the studied spherules. These spherules contain olivines of various sizes nested in glass groundmass dominated by Ca, Fe, Al and Si. In addition, various types of olivines are classified texturally (Genge et al., 2016). They are also identified in the present collection, such as cumulative olivine cosmic spherules with characteristic properties of increment of olivine sizes from one side of the spherule to another. Skeletal porphyritic spherules are characterized by elongated coarse-grain olivines. Certain parts of MMs undergo partial melting where relict grain can be preserved. Relict olivines are observed in ~ 5 % of cosmic spherules, and

these relict olivines are essential for forsterite composition. As relict, olivines escape melting and thus are very useful in ascertaining the particle's precursors and pre-atmospheric chemistry.

3.1.2 Barred, Cryptocrystalline and Glass type spherules

Barred, cryptocrystalline, and glass-type cosmic spherules are relatively homogenous compared to the other types. Barred cosmic spherules dominate all different types in the present collection and represent ~53% of the total sample analysed. Glass and cryptocrystalline cosmic spherules quantity are identical, and each constitutes around 6% in the present collection. Glass cosmic spherules have suffered more atmospheric heating as compared to the cryptocrystalline and barred cosmic spherules. Barred olivine cosmic spherules generally form around ~1900 K, while cryptocrystalline and glass are formed at around ~2000 K and ~2300 K, respectively (Rudraswami et al., 2022). Barred olivine (BO) cosmic spherules have characteristically parallel-arranged olivine grains within glassy mesostasis and elongated parallel bars visible in polished sections (Fig.3a). Cryptocrystalline (CC) spherules are composed dominantly of submicron crystallites.

3.1.3 Scoriaceous cosmic spherules

Scoriaceous MMs are characterised by their vesicular properties formed due to escaping of volatile phases during atmospheric entry. Here in the present study, only three particles are scoriaceous. These particles are predominantly micro porphyritic olivine mesostasis with crystal sizes <1 μm within an interstitial silicate glass phase.

3.1.4 G-type and I-type cosmic spherules

G-type cosmic spherules exhibit typical textures featuring magnetite dendrites dominated within a mesostasis of silicate glass. The chemical composition of G-type spherules falls intermediate between nearly chondritic silicate type and I-type cosmic spherules. Two G-type cosmic spherules are found here, and I-type represents ~10% of the present collection. I-type cosmic spherules are either produced by melting due to frictional heating during atmospheric entry and are mainly composed of iron oxides and Fe-Ni metal, or the metal particle released as a bead from a silicate chondritic body gets oxidised during entry into the Earth's atmosphere (Rudraswami et al., 2014b).

4. Discussion

4.1 Bulk chemistry and contributing precursors

The bulk composition of cosmic spherules was determined carefully by averaging multiple beam spots analysed using an electron microprobe. Bulk major elemental ratio normalized to Si and

CI chondrite for various types of cosmic spherules have been presented in (Fig.5). The compilation of the chemical composition of all the studied spherules is provided in Appendix A. Depletion in S, Na and Fe, as compared to bulk CI is observed and suggests their loss during atmospheric entry due to their high volatility. The Mg content of cosmic spherules broadly matches the CI chondritic values. The Cr, Mn and Al values are observed to be higher, probably due to their refractory nature. In contrast, Ca and Ni values show both trends indicating heterogeneity of precursors and weathering effect. Unlike unmelted MMs, where pyroxene is a dominant mineral along with olivine (Kurat et al., 1994; Rudraswami et al. 2018b), in the case of cosmic spherules, pyroxene is less abundant. However, pyroxene can be observed in some cosmic spherules which have not experienced extreme heating (Rudraswami et al. 2018b). Among the collected micrometeorite particle SSD48 DSS 02 P38 (Fig. 3i), which is around 270 μm in diameter, is predominantly composed of pyroxene and very fine randomly oriented metal veins. The spherule has many cracks throughout, which seems to be primary as metal veins cross-cut the cracks indicating they are relatively older than the veins. The pyroxene is low Ca-pyroxene ($\text{En}=82.68$, $\text{Fs}=16.59$ and $\text{Wo}=0.73$). The preservation of pyroxene mineralogy indicates that the atmospheric heating effect has not affected the particle. The particle is of a crescent shape, with a big round void, probably due to the ejection of material during atmospheric entry. The particle is also affected by etching and has irregular voids close to the edge of the particle.

Some glass spherules have nearly pyroxene normative composition (Rudraswami et al., 2012). This may be due to unfavourable, kinetically conducive conditions and the limitation of crystallisation time during atmospheric entry. Recrystallised pyroxene crystals are absent in the case of cosmic spherules. In case pyroxene is found in cosmic spherule, it must be of primary origin and have not been formed due to recrystallisation in the terrestrial atmosphere. The occurrence of pyroxene crystals in cosmic spherule reflects atmospheric entry conditions, and their presence indicates high zenith angles ($\sim 70^\circ$ – 90°) and low entry velocity ($< 16\text{km/s}$) with temperature not exceeding $\sim 1870\text{ K}$ (Rudraswami et al., 2018b).

Olivine is a significant component in MMs, and here in the present collection of cosmic spherules, various olivine morphologies are observed. Representative BSE images are shown in (Fig. 6). Broadly, olivines are formed by the dynamic crystallisation of melt produced during atmospheric entry. However, certain relict olivines are present, most of which are Mg-rich. Relict olivines are not formed by the crystallisation of partial melt during atmospheric entry. They are essential in deciphering parent bodies and can be recognised by their distinctive Z contrast, morphology and often association with Fe-Ni metals. (Steele et al., 1986; Rudraswami et al., 2016) The chemical

compositions of the studied porphyritic and relict olivines are provided in Appendix B. The forsterite abundance of porphyritic and relict olivines is shown in (Fig.7). It is observed that porphyritic olivines have a more comprehensive composition range of Fo₁₃₋₉₆, with the majority of them falling in the range of Fo₇₅₋₈₅. In contrast, relict olivines show a narrow range with Fo₈₈₋₉₉, with most having Fo_{>95}. Also, the refractory nature of olivines increases with Mg content, thus, the chances of survival of relict forsterite. The variable shapes and chemistry of olivines, either overgrown on the relict olivine phase or newly recrystallised porphyritic olivine, suggest a gradient of temperature and cooling rate. These observations annul the homogenous heating of particles during atmospheric entry and suggest variable temperature gradient across the particle, which is controlled by its shape, rotation and angle of entry. Different secondary olivines formed during atmospheric entry display various shapes and textures; their textural property is mainly controlled by cooling rate and melt viscosity (Donaldson et al., 1976). The most common shapes of olivines observed in porphyritic cosmic spherules are granular, skeletal, platy shaped, dendritic, and zoned (Fig. 6). Also, Genge et al. (2016) depending upon the distribution of olivine size and morphologies present in cosmic spherules has subdivided cosmic spherules as cumulative olivine cosmic spherules and non-cumulative. In the case of cumulative olivine cosmic spherules, olivine phenocryst size increases from one side of the spherule to the other (Fig. 6c, d). Individual olivines are also separately analysed. Their elemental composition is compared with olivine composition found in known meteorite classes (Fig. 8). It is observed that most of the relict olivine composition mainly belongs to carbonaceous chondrites (Rudraswami et al., 2020). Also, it is noted that porphyritic olivine and relict olivine can be clearly distinguished by observing their FeO content as they show large variations in FeO content as compared to relict olivines.

Determination of the cosmic spherule progenitors is a significant challenge as textural and chemical modification occurred during atmospheric entry. Also, MMs represent the fragment of different components of meteorites such as chondrule, matrix, Calcium Aluminium Inclusions (CAIs), isolated grains, etc (Genge et al., 2005; Taylor et al. 2010; Soens et al., 2020). As a result, identifying the parent body from these small bodies is challenging, nonetheless is important to understand the nature of the dust production and dynamic behaviour of celestial bodies and their transportation towards the Earth.

The bulk elemental compositions of these different S-type cosmic spherules can be applied to explore their relationship with their possible meteorite parent bodies. The histograms (Fig. 9) depict elemental ratios (Al/Si, Mg/Si, and Fe/Si) normalised to CI values and are compared with various carbonaceous and ordinary chondrites. The Al/Si values for carbonaceous (CI, CM, CO, CV)

chondrites are close to or slightly greater than 1, but decline for ordinary and enstatite chondrites. Mg/Si and Fe/Si also show a similar trend. The cosmic spherules were subjected to severe frictional heating during atmospheric entry, obliterating their chemical compositions. Some cosmic spherules have partially melted textures, such as scoriaceous and relict grain bearing (RGB) that may be easy to relate with their precursors compared to more heated barred, glass and cryptocrystalline spherules. In cosmic spherules, Fe, Si, and Mg are major elemental components, among which the Fe evaporation rate is very high compared to Si, followed by Mg (Hashimoto, 1983; Rudraswami et al., 2015). The CaO and Al₂O₃ are refractory and generally do not show signatures of vaporisation as suggested by heating experiments (Hashimoto, 1983). Si evaporation rate is depicted to be around three times more than Mg. The heating effect should be kept in consideration while predicting precursors. The Fe is volatile and is reflected as a decrease in Fe/Si ratio. Si has greater volatility than Mg; the Si vaporisation increases Mg/Si value. Mg mainly compensates for the loss of Fe as compared to Si. If we predict precursor by Al/Si value, cosmic spherules have a meagre contribution from CV chondrites. However, this is not the case with Mg/Si and Fe/Si. During atmospheric entry heating effect, they are modified and thus becomes difficult to relate these cosmic spherules to a particular chondritic precursor. Further, Fe-Mg-Mn systematic can discriminate between achondrite and chondritic parent bodies. Fe/Mg and Fe/Mn ratios of glass cosmic spherules lie in the chondritic region (Fig. 10). However, the proportion contributed by the achondritic parent body is very minimal and reported by few researchers (Taylor et al., 2007; Gounelle et al., 2009; Soens et al., 2022). The CaO and faylitic content of relict olivines (Fig. 11) suggests that most of them belong to type I chondrules (Mg# > 0.9) of carbonaceous chondrites. The dominance of carbonaceous chondrites as a source for MMs over ordinary chondrites indicates that meteoritic flux can be attributed to their fragile, hydrous and porous carbonaceous chondritic nature that can produce more dust during asteroidal collisions (Rudraswami et al., 2018a; Taylor et al., 2012).

4.2 Interaction with the terrestrial atmosphere

The micrometeoroids entering the Earth's atmosphere suffer severe heating, and the degree of heating is reflected in texture and chemical composition (Toppani et al., 2001; Rudraswami et al., 2015). While unmelted MMs are the least affected, cosmic spherules show alteration in their original textures and mineralogy. However, they provide important clues about the processes that occurred during atmospheric entry, such as loss of volatile elements, degree of ablation, reprocessing of original textures, mineralogy, and partial melting. The vesicles observed in scoriaceous MMs (Fig. 3g) are produced due to escaping of volatiles during atmospheric entry. An understanding of the effect of heating is essential for inferring orbital parameters and source bodies of incoming dust. The

degree of heating is controlled by various entry parameters such as particle size, velocity, entry angle, and density (Rudraswami et al., 2015, 2016; Carrillo- Sánchez et al., 2020). A thin magnetite rim formed due to oxidation during atmospheric entry is observed in most of these spherules. Certain textural features such as dendritic magnetite and dagger-shaped magnetite (Fig. 12c, d) endorse sudden quenching of the melt generated due to frictional heating. In addition, the melted patch (Fig.12a, b), with the feathery appearance of the magnetic phase suggesting the separation of the silicate phase and metallic content, demonstrates melting during atmospheric entry. Sometimes due to density contrast and spin, the metal phase is separated (Fig.12e, f) as a bead which may also eject in some cases. This texture can be utilised to ascertain the leading face during atmospheric deceleration.

As MMs are extraterrestrial dust produced by asteroidal collisions and sublimation of comets, the MMs may show different textures and mineralogy even though they belong to the same parent body as they can be part of a chondrule, matrix or individual fragments of the meteoroid. Thus, the abundance and relative proportion of matrix, anhydrous mineral phases and chondrules, which vary within different classes of meteorites, constrain the nature of extraterrestrial dust reaching the Earth. Taylor et al. (2012) discussed that matrix-dominated micrometeoroids would produce a different texture sequence upon heating than matrix-poor micrometeoroids. Some olivines in the present study show zoning effect due to disequilibrium crystallisation from melts produced as a result of calefaction because of frictional heat generated while entering into the terrestrial atmosphere. Various olivine morphologies and their minor elemental content attest to information regarding the cooling history and behaviour of melt during interaction with the terrestrial atmosphere.

Individual zoned crystals are analysed, and chemical variation from core to the rim is observed for commonly present elemental oxides viz FeO, MgO, MnO, SiO₂, Al₂O₃, and CaO (Fig. 13). In most of the zoned spherules core has been least affected as compared to outer marginal part. It is observed that FeO and SiO₂ show opposite trends, and MgO is higher in the core and decreases towards the rim. In contrast, FeO and SiO₂ are higher in the marginal part and decrease toward the core. The ablation of FeO is observed to be higher than SiO₂, CaO, MnO, and Al₂O₃. CaO and Al₂O₃ do not follow any specific trend suggesting their relatively refractory nature compared to FeO and SiO₂ and compositional diversity in dust-producing bodies. Chemical zoning reflects the thermal history of the mineral and melt. Genge et al. (2016) concluded that cumulate porphyritic spherules enter at a higher velocity than non-cumulate coarse-grained porphyritic olivine spherules; thus shapes and nature of olivine crystals may constrain the entry velocity of the micrometeoroid. Different orientation of olivines as observed in the collection may be attributed to the spinning of the

melt from which olivine crystallisation is taking place (Fig. 6). The equant crystals at the margin of the cosmic spherule as compared to the central part may be related to entry angle and spinning favouring crystallisation nucleus to migrate towards the margin. While in case of cosmic spherules having equidimensional crystals of olivine distributed uniformly throughout the spherule can be attributed to the limited spinning effect and homogenous distribution of crystallisation nuclei throughout the cosmic spherules.

Olivines show a variety of NiO contents. Higher NiO contents of olivines (>1 wt.%) in cosmic spherules have been interpreted as indicating a Fe, Ni metal-rich, C-poor precursor by Cordier et al. (2011). This variability could reflect different proportions between Fe, Ni metal grains and silicate in their precursors or different oxidising conditions during their penetration of the Earth's atmosphere. The Ni content of olivines is plotted in (Fig. 14). It is easy to identify relict olivines which were not melted and affected due to frictional heat during atmospheric entry, and are found to be Ni-poor. The concentration of NiO in such minerals is less than 0.5 wt. %. In contrast, in the case of thermally affected olivines, the range may reach up to 5–6 wt. %. However, most of them fall within 1wt. %. The presence of Ni in olivine is controlled by various factors such as temperature, oxygen fugacity and melt composition. The carbon content in the precursor that generates reducing conditions upon pyrolysis also affects the oxygen fugacity. While the atmospheric passage recrystallised olivines are formed by disequilibrium crystallisation, undercooling is very fast. In contrast, melt generated from ordinary chondritic precursors lacking carbon will generate oxidising conditions. The reducing conditions will favour the separation of metal and sulfide phases within silicate melt. This will lead to the segregation of Fe, Ni and Co and the development of Ni-poor olivines. In contrast, oxidising conditions will favour the formation of Ni-rich olivine. Also, the high variability of Ni in the recrystallised olivines suggests variable conditions mentioned above formed due to heterogeneous precursors and variable entry parameters.

4.3 Interaction with seawater

Seawater interaction with cosmic spherules is essential to constrain weathering effects and dissolution of cosmic spherules altering their original mineralogy. To shed light on precursors, it becomes vital to understand the changes occurring due to seawater interaction. Compared to MMs recovered from Polar Regions, deep-sea cosmic spherules are heavily affected by ocean water and show etching and poor preservation, however, collection from deep-sea sediments provides a window of longer time frame in comparison to Polar collections. The extent of dissolution of extraterrestrial material and etching also depends on the duration of residence of cosmic spherules in the ocean water column and pH conditions. A study (Uścińowicz, 2012) on two cores collected from

the Pacific Ocean found that spherules in deeper cores are in poor condition compared to spherules collected from the upper portion of the cores. Weathering of MMs can be reflected in several morphological characteristics such as cavities, etch pits, infilled cavities, replaced silicate and hydrated metal phases (Van Ginneken et al., 2016). Different mineral phases are affected differently. Silicates are leached more prominently, while metal phases such as magnetite are more resistant, as can be seen in (Fig.15). Here we can observe variable dissolution rims (Fig. 15 a, b) where the etching of marginal portion is revealed by preferential loss of unstable silicate phases as compared to metallic phases. The intact core portion suggests in most of the preserved spherules etching starts from the surface and gradually goes into the deeper portion. However, due to the differential resistance of various phases of dissolution with seawater, spherules appear crumbled. Barred cosmic spherules show long deep grooves formed due to the etching of glassy material between olivine laths (Fig.15 c). In the case of porphyritic olivine cosmic spherules, the selective dissolution of olivines creates a honeycomb texture where olivine phases are readily dissolved compared to surrounding phases (Fig. 15d-f). Etch pits of variable shapes are seen due to the preferred selective dissolution of silicate phases (Fig. 15 g, h). The scoriaceous and I-type cosmic spherules here show minimum etching. However, as we got only three scoriaceous particles, it shows the possibility of complete dissolution of scoriaceous particles where vesicles may have increased vulnerability of particles due to increment in the exposed surface area towards dissolution and thus practically making them most etched particles. The glass spherules are relatively homogenous and show less etching than barred and porphyritic cosmic spherules.

4.4 Implications for ocean Biogeochemistry

Being the largest reservoir for incoming extraterrestrial material, the biogeochemistry of the ocean is affected by the input of elements, particularly for those which have a meagre concentration in the terrestrial reservoir such as PGE and solar wind implanted ^3He . The contribution of the incoming extraterrestrial dust to the ocean can be from condensed meteoric smoke generated during atmospheric entry and dissolution of the surviving portion. The chondrites which seem to dominate the precursor of cosmic spherules have multifold concentrations of PGE as compared to the continental crust(Ru~ 645 times, Rh ~245 times, Pd~ 225times, Os~12,250, Ir~ 11,375 times and Pt ~673). The presence of elevated concentrations of refractory metals including PGE in cosmic spherules can be attributed to oxidation and differentiation when spherules are melted due to heat generated during atmospheric entry (Brownlee et al., 1984; Rudraswami et al., 2014a, b; Savelyev et al., 2022).

In the case of ^3He , studies (Merrihue, 1964; Ozima and Podosek, 1983; Ozima et al., 1984) have shown that deep ocean sediments show elevated $^3\text{He}/^4\text{He}$ values (up to around 20,000 times average $^3\text{He}/^4\text{He}$ of continental crust). This elevated signature of Helium isotope can be attributed to the contribution from extraterrestrial dust and can be applied for the better estimation of growth rates of ferromanganese nodules and sedimentation rate with a benefit over measurement carried out over radioactive species as it is not affected by half-life (Li et al., 2002). Also, the ferromanganese crust in the deep ocean, owing to its very slow growth rates (<10 mm/Ma) are promising reservoir for a high number of cosmic spherules (Savelyev et al., 2022). In addition, there is a possibility that during subduction of oceanic sediments containing signatures of extraterrestrial noble gas (He and Ne) contributed by extraterrestrial dust can affect mantle geochemistry (Anderson, 1993; Schwarz et al., 2005). Further studies are needed in this direction to constrain the contribution of extraterrestrial components through subduction. Extraterrestrial dust may play an important role in driving primary productivity in the ocean by supplying bioavailable iron, especially in high nutrient low chlorophyll (HNLC) regions receiving meagre input from Aeolian dust such as Southern Ocean (Johnson et al., 2001; Renier and Turchyn, 2018; Rudraswami et al., 2021). If we compare the percentage of I-type cosmic spherules in the current study with those of polar collections (Maurette et al., 1991; Taylor et al., 2000; Goderis et al., 2020; Genge et al., 2020; Rudraswami et al., 2020) it comes nearly 2 to 5 times. This is due to the preferential dissolution of S-type cosmic spherules increasing the I-type to S-type ratio in the deepsea collection. Subsequently, if we compare the flux estimated by various workers using cosmic spherules in deepsea sediments (Murrel et al., 1980 ~90 t/a; Prasad et al., 2013 ~160 t/a) is contrastingly low when compared with flux calculation done in polar region (Yiou et al., 1991 ~1500 t/a; Taylor et al., 1998~ 2700 t/a; Yada et al., 2004~ 1100 t/a). Considering the homogenous distribution of incoming extraterrestrial dust, contrastingly low flux estimated in deepsea regions is attributed to dissolution and this dissolved portion may contribute to the inventory of the bioavailable iron in the ocean. If we compare the flux calculation carried out by using Os measurement in deepsea sediments by Peucker-Ehrenbrink and Ravizza (2000), which is 30,000 t/a, it matches with the flux calculation done by Love and Brownlee (1993) suggesting contribution through an ablated portion of extraterrestrial dust. Meteoric smoke produced during atmospheric entry may provide ocean surface bioavailable iron as a slowly settling recondensed nanometric smoke. Also, as we have seen, olivine is the most dominant phase in MMs. They are the most unstable orthosilicate for dissolution studies like Montserrat et al. (2017) which suggests that the dissolution of olivines may increase the alkalinity of seawater and can have a significant role in CO_2 drawdown. Thus it is evident that although the quantity of extraterrestrial dust is very less as compared to terrestrial sedimentation, it plays a vital role in the biogeochemistry of the Oceans and

the interaction of extraterrestrial dust with ocean water columns should be evaluated in detail in future studies.

5. Conclusions

The present study discusses preliminary results throwing light on the chemical composition of cosmic spherules recovered from the Central Indian Ocean basin (CIOB). These spherules will add to the inventory of extraterrestrial material. Due to better preservation and concentration, most recent micrometeorite collections focus on the Polar region. However, the deep-sea region with a meagre sedimentation rate and far from anthropogenic activity and terrestrial sediment influx is an important source of these extraterrestrial particles. Their study is also vital to constrain the geochemical budget, especially PGE. Interaction with seawater and its endurance is vital to shed light on preserving extraterrestrial flux in the ocean. The present studied cosmic spherules are chemically analysed, and in the present study, their mineralogy is utilised to relate them with possible known precursors. The spherules can be linked to carbonaceous chondrites, which are among the most primitive material present in the solar system. However, the frictional heat and ocean water extirpate the mineralogy and textures, impeding the identification of precursors. The effect of heating during atmospheric entry creates zoning in olivines. The elemental ratio variation within zoned crystals suggests that FeO and SiO₂ are more sensitive to heating than more refractory CaO and Al₂O₃. A clear distinction is observed in Ni content in porphyritic and relict olivines and can be attributed to atmospheric heating. Also, the olivine morphologies and their distribution within the particle are constrained by the precursor mineralogy, spinning, and the peak temperature generated during deceleration. In addition, the dissolution of these particles may significantly affect global climate, and thus, the impetus may be given to understanding the interaction of ocean water and extraterrestrial dust.

Acknowledgement

This work is supported by GAP2175 (MOES-PMN) and Respond-ISRO (GAP3332) projects. This is NIO's contribution number, XXXX.

Supplementary Material

Appendix A

Chemical compositions of the studied cosmic spherules.

Appendix B

Chemical compositions of the studied porphyritic and relict olivines

References

- Akulov, N., Pavlova, L.A., Antipin, E.V., 2014. Geochemical peculiarities of micrometeorites in bottom sediments of Lake Baikal. *Doklady. Earth Science*. 454, 193-198.
- Anderson, D.L., 1993. Helium-3 from the mantle: primordial signal or cosmic dust? *Science*. 261,170-176.
- Beckerling, W., Bischoff, A., 1995. Occurrence and composition of relict minerals in micrometeorites from Greenland and Antarctica - implications for their origins. *Planet. Space Sci.* 43, 435-449.
- Bi, D., Morton, R.D., Wang, K., 1993. Cosmic nickel-iron alloys spherules from Pleistocene; sediments, Alberta, Canada. *Geochimica et Cosmochimica Acta*. 57, 4129-4136.
- Blanchard, M., Brownlee, D., Bunch, T., Hodge, P., Kyte, F., 1980. Meteoroid ablation spheres from deep-sea sediments. *Earth Planet. Sci. Lett.* 46, 178-190.
- Bottke Jr, W.F., Vokrouhlický, D., Rubincam, D.P., Nesvorný, D., 2006. The Yarkovsky and YORP effects: Implications for asteroid dynamics. *Annu. Rev. Earth Planet. Sci.* 34, 157-91.
- Brearley, A.J., Jones, R.H., 1998. Chondritic meteorites. In *Planetary materials*, edited by Papike J. J. *Reviews in Mineralogy*, Washington, D.C. Mineralogical Society of America. 36, 1-398.
- Briani, G., Pace, E., Shore, S.N., Pupillo, G., Passaro, A., Aiello, S., 2013. Simulations of micrometeoroid interactions with the Earth atmosphere. *Astronomy & Astrophysics*. 552, A53.
- Brownlee, D.E., Bates, B., Schramm, L., 1997. The elemental composition of stony cosmic spherules. *Meteorit. Planet. Sci.* 32, 157-175.
- Brownlee, D. E., Bates, B. A., Wheelock, M. M., 1984. Extraterrestrial platinum group nuggets in deep-sea sediments. *Nature*. 309(5970), 693-695.
- Bruun, A.F., Langer. E., Pauly, H., 1955. Magnetic particles found by raking the deep sea bottom. *Deep Sea Research*. 2(3), 230-46.
- Carrillo-Sánchez, J.D., Gómez-Martín, J.C., Bones, D.L., Nesvorný, D., Pokorný, P., Benna, M., Flynn, G.J., Plane, J.M., 2020. Cosmic dust fluxes in the atmospheres of Earth, Mars, and Venus; *Icarus*. 335, 113395.
- Cordier, C., Folco, L., Suavet, C., Sonzogni, C., Rochette, P., 2011. Major, trace element and oxygen isotope study of glass cosmic spherules of chondritic composition: The record of their source material and atmospheric entry heating. *Geochim. Cosmochim. Acta*. 75, 5203–5218.
- Donaldson, C.H., 1976. An experimental investigation of olivine morphology. *Contributions to Mineralogy and Petrology*. 57(2), 187-213.
- Duprat, J., Engrand, C., Maurette, M., Kurat, G., Gounelle, M., Hammer, C., 2007. Micrometeorites from central Antarctic snow: The CONCORDIA collection. *Advances in Space Research*. 39(4), 605-611.

- Finkelman, R. B., 1970. Magnetic particles extracted from manganese nodules: Suggested origin from stony and iron meteorites. *Science*. 167(3920), 982-984.
- Flynn, G. N., 1989. Atmospheric entry heating: A criterion to distinguish between asteroidal and cometary sources of interplanetary dust. *Icarus*. 77, 287-310.
- Genge, M. J., Van Ginneken, M., Suttle, M. D., 2020. Micrometeorites: Insights into the flux, sources and atmospheric entry of extraterrestrial dust at Earth. *Planetary and Space Science*. 187, 104900.
- Genge, M. J., Larsen, J., Van Ginneken, M., & Suttle, M. D., 2017. An urban collection of modern-day large micrometeorites: Evidence for variations in the extraterrestrial dust flux through the Quaternary. *Geology*. 45(2), 119-122.
- Genge, M.J., Suttle, M., Van Ginneken, M., 2016. Olivine settling in cosmic spherules during atmospheric deceleration: An indicator of the orbital eccentricity of interplanetary dust. *Geophysical Research Letters*. 43(20), 10-646.
- Genge, M.J., Engrand, C., Gounelle, M., Taylor, S., 2008. Classification of micrometeorites. *Meteorit. Planet. Sci.*, 43, 497-515.
- Genge, M.J., Gileski, A., Grady, M.M., Chondrules in Antarctic micrometeorites; 2005 *Meteoritics & Planetary Science*. 40(2), 225-38
- Genge, M. J., Grady, M.M., Hutchison, R., 1997. The textures and compositions of fine-grained Antarctic micrometeorites: Implications for comparisons with meteorites. *Geochim. Cosmochim. Acta*. 61, 5149-5162.
- Goderis, S., Soens, B., Huber, M. S., McKibbin, S., Van Ginneken, M., Van Maldeghem, F., & Claeys, P., 2020. Cosmic spherules from Widerøefjellet, Sør Rondane Mountains (East Antarctica). *Geochim. Cosmochim. Acta*. 270, 112-143.
- Gounelle, M., Chaussidon, M., Morbidelli, A., Barrat, J.A., Engrand, C., Zolensky, M.E., Mckeegan, K.D., 2009. Unique basaltic micrometeorite expands the inventory of solar system planetary crusts. *Proceedings of the National Academy of Sciences*. 106(17), 6904-6909.
- Hashimoto, A., 1983. Evaporation metamorphism in the early solar nebula-evaporation experiments on the melt FeO-MgO-SiO₂-CaO-Al₂O₃. *Geochim. J.* 17, 111-145.
- Johnson, K.S., 2001. Iron supply and demand in the upper ocean: Is extraterrestrial dust a significant source of bioavailable iron? *Global Biogeochemical Cycles*. 15(1), 61-63.
- Jones, R.H., Carey, E.R., 2006. Identification of relict forsterite grains in forsterite-rich chondrules from the Mokoia CV3 carbonaceous chondrite. *American Mineralogist*. 91(10), 1664-1674.
- Kurat, G., Koerberl, C., Presper, T., Brandstatter, E.F., Maurette, M., 1994. Petrology and geochemistry of Antarctic micrometeorites. *Geochim. Cosmochim. Acta* 58, 3879-3904.

- Kurat, G., Mayr, M., Ntaflos, T., Graham, A.L., 1989. Isolated olivines in the Yamato 82042 CM2 chondrite: The tracing of major condensation events in the solar nebula. *Meteoritics*. 24(1), 35-42.
- Li, Y., Song, H., Li, J., 2002. Extraterrestrial ^3He in marine polymetallic nodules: A potential method for measuring growth rate of nodules. *Science in China Series B: Chemistry*. 45, 38-46.
- Love, S. G., Brownlee, D. E., 1993. A direct measurement of the terrestrial mass accretion rate of cosmic dust. *Science*. 262, 550–553.
- Love, S. G., Brownlee, D. E., 1991. Heating and thermal transformation of micrometeoroids entering the Earth's atmosphere. *Icarus*. 89, 26-43.
- Marvin, U.B., Einaudi, M.T., 1967. Black, magnetic spherules from Pleistocene and recent beach sand. *Geochimica et Cosmochimica Acta*. 31(10), 1871-1884.
- Maurette, M., Olinger, C., Michel-Levy, M.C., Kurat, G., Pourchet, M., Brandstätter, F. Bourot-Denise, M., 1991. A collection of diverse micrometeorites recovered from 100 tonnes of Antarctic blue ice. *Nature*. 351(6321), 44-47.
- Maurette, M., Jehanno, C., Robin, E., Hammer, C., 1987. Characteristics and mass distribution of extraterrestrial dust from the Greenland ice cap. *Nature*. 328, 699-702.
- Merrihue, C., 1964. Rare gas evidence for cosmic dust in modern Pacific red clay. *Annals of the New York Academy of Sciences*. 119, 351-367.
- Montserrat, F., Renforth, P., Hartmann, J., Leermakers, M., Knops, P., Meysman, F.J., 2017. Olivine dissolution in seawater: implications for CO₂ sequestration through enhanced weathering in coastal environments. *Environmental science & technology*. 51(7), 3960-3972.
- Murray, J., Renard, A.F., 1891. Report on deep-sea deposits based on the specimens collected during the voyage of HMS Challenger in the years 1872 to 1876. HM Stationery Office.
- Murrell, M.T., Davis Jr, P.A., Nishiizumi, K., Millard Jr, H.T., 1980. Deep-sea spherules from Pacific clay: Mass distribution and influx rate *Geochimica et Cosmochimica Acta*. 44(12), 2067-2074.
- Nakamura, T., Imae, N., Nakai, I., Noguchi, T., Yano, H., Terada, K., Murakami, T., Fukuoka, T., Nogami, K.I., Ohashi, H., Nozaki, W., 1999. Antarctic micrometeorites collected at the Dome Fuji Station. *Antarctic Meteorite Research*. 12, 183.
- Noguchi, T., Ohashi, N., Tsujimoto, S., Mitsunari, T., Bradley, J.P., Nakamura, T., Toh, S., Stephan, T., Iwata, N., Imae, N., 2015. Cometary dust in Antarctic ice and snow: Past and present chondritic porous micrometeorites preserved on the Earth's surface. *Earth and Planetary Science Letters*. 410, 1-11.
- Ozima, M., Takayanagi, M., Zashu, S. et al., High $^3\text{He}/^4\text{He}$ ratio in ocean sediments, *Nature*, 1984, 311: 448-450.
- Ozima, M., Podosek, F. A., 1983. *Noble Gas Geochemistry*, New York: Cambridge Univ. Press.

- Parkin, D.W., Tilles, D., 1968. Influx Measurements of Extraterrestrial Material: Sea sediments, polar ice, air, and space are searched for amount and character of interplanetary debris. *Science*. 159(3818), 936-946.
- Peucker-Ehrenbrink, B., Ravizza, G., 2000. The effects of sampling artefacts on cosmic dust flux estimates: A revaluation of non volatile tracers (Os, Ir). *Geochim. Cosmochim. Acta*. 64, 1965-1970.
- Plane, J. M. , 2012. Cosmic dust in the earth's atmosphere. *Chemical Society Reviews*. 41(19), 6507-6518.
- Prasad, M.S., Rudraswami, N.G., De Araujo, A., Babu, E.V., Vijaya Kumar, T., 2015. Ordinary chondritic micrometeorites from the Indian Ocean. *Meteoritics & Planetary Science*. 50(6), 1013-31.
- Prasad, M. S., Rudraswami, N. G., Panda, D. K., 2013. Micrometeorite flux on Earth during the last 50,000 years. *Journal of Geophysical Research*. 118, 2381-2399.
- Reiners, P.W., Turchyn, A.V., 2018. Extraterrestrial dust, the marine lithologic record, and global biogeochemical cycles. *Geology*. 46(10), 863-866.
- Rochette, P., Folco, L., Suavet, C., Van Ginneken, M., Gattacceca, J., Perchiazzi, N., Braucher, R., Harvey, R.P., 2008. Micrometeorites from the Transantarctic Mountains. *Proceedings of the National Academy of Sciences*. 105(47), 18206-18211.
- Rubin, A.E., Grossman, J.N., 2010. Meteorite and meteoroid: New comprehensive definitions. *Meteoritics & Planetary Science*. 45(1), 114-122.
- Rudraswami, N.G., Pandey, M., Fernandes, D., Carrillo-Sánchez, J.D., Feng, W., Plane, J.M.C. Singh, V.P., 2022. Oxygen ablation during atmospheric entry: Its influence on the isotopic composition of micrometeorites. *Astrophysical Journal*, 940(1), 25.
- Rudraswami, N.G., Pandey, M., Genge, M.J., Fernandes, D., Brownlee, D., 2021. Extraterrestrial dust as a source of bioavailable iron contributing to the ocean for driving primary productivity. *Meteoritics and Planetary Science*. 56(12), 2175-2090.
- Rudraswami, N. G., Fernandes, D., Pandey, M., 2020. Probing the nature of extraterrestrial dust reaching the Earth's surface collected from the Maitri station, Antarctica. *Meteoritics & Planetary Science*. 55, 2256–2266.
- Rudraswami, N.G., Fernandes, D., Naik, A.K., Prasad, M.S., Carrillo-Sánchez, J.D., Plane, J.M.C., Feng, W., Taylor, S., 2018a Selective disparity of ordinary chondritic precursors in micrometeorite flux; *Astrophysical Journal* 853 38.
- Rudraswami, N.G., Fernandes, D., De Araujo. A., Shyam Prasad, M., Taylor, S., 2018b. Perceptive of the pyroxene-bearing micrometeorites and their relation to chondrites. *Meteoritics & Planetary Science*. 53(10), 2035-2050.
- Rudraswami, N.G., Prasad, M.S., Dey, S., Fernandes, D., Plane, J.M.C., Feng, W., Taylor, S. Carrillo-Sánchez, J.D., 2016. Relict olivines in micrometeorites: Precursors and interactions in the Earth's atmosphere. *The Astrophysical Journal*. 831(2), 197.

- Rudraswami, N.G., Prasad, M.S., Dey, S., Plane, J.M.C., Feng, W. Taylor, S., 2015. Evaluating changes in the elemental composition of micrometeorites during entry into the Earth's atmosphere. *Astrophysical Journal*. 814, 78.
- Rudraswami, N. G., Prasad, M. S., Plane, J. M. C., Berg, T., Feng, W., Balgar, S. 2014a. Refractory metal nuggets in different types of cosmic spherules. *Geochimica et Cosmochimica Acta*. 131, 247-266.
- Rudraswami, N. G., Prasad, M. S., Babu, E. V. S. S. K., & Kumar, T. V., 2014b. Chemistry and petrology of Fe–Ni beads from different types of cosmic spherules: Implication for precursors. *Geochimica et Cosmochimica Acta*. 145, 139-158.
- Rudraswami, N. G., Prasad, M. S., Babu, E. V. S. S. K., Kumar, T. V., Feng, W., Plane, J. M. C., 2012. Fractionation and fragmentation of glass cosmic spherules during atmospheric entry. *Geochimica et Cosmochimica Acta*. 99, 110-127.
- Rudraswami, N. G., Ushikubo, T., Nakashima, D., Kita, N. T., 2011. Oxygen isotope systematics of chondrules in the Allende CV3 chondrite: High precision ion microprobe studies. *Geochimica et Cosmochimica Acta*. 75(23), 7596-7611.
- Russell, S. D. J., Longstaffe, F. J, King, P. L, Larson, T. E., 2010. The oxygen-isotope composition of chondrules and isolated forsterite and olivine grains from the Tagish Lake carbonaceous chondrite. *Geochimica et Cosmochimica Acta*. 74(8), 2484-2499.
- Savelyev, D. P., Savelyeva, O. L., Moskaleva, S. V., Rashidov, V. A., 2022. Composition of Cosmic Spherules from Ferromanganese Crusts of the Magellan Seamounts. *Geochemistry International*. 60(5), 411-420.
- Schwarz, W. H., Trieloff, M., Altherr, R. 2005. Subduction of solar-type noble gases from extraterrestrial dust: constraints from high-pressure low-temperature metamorphic deep-sea sediments. *Contributions to Mineralogy and Petrology*. 149, 675-684.
- Soens, B., Chernozhkin, S. M., de Vega, C. G., Vanhaecke, F., Van Ginneken, M., Claeys, P., & Goderis, S., 2022. Characterization of achondritic cosmic spherules from the Widerøefjellet micrometeorite collection (Sør Rondane Mountains, East Antarctica). *Geochimica et Cosmochimica Acta*. 325, 106-128.
- Soens, B., Suttle, M.D., Maeda, R., Vanhaecke, F., Yamaguchi, A., Van Ginneken, M., Debaille, V., Claeys, P., Goderis, S., 2020. Evidence for the presence of chondrule- and CAI-derived material in an isotopically anomalous Antarctic micrometeorite. *Meteoritics & Planetary Science*. 12, 2703-26.
- Steele, I.M., 1992 Olivine in Antarctic micrometeorites: Comparison with other extraterrestrial olivine. *Geochimica et Cosmochimica Acta*. 56(7), 2923-2929.
- Steele, I.M., 1986. Compositions and textures of relic forsterite in carbonaceous and unequilibrated ordinary chondrites. *Geochimica et Cosmochimica Acta*. 50(7), 1379-1395.
- Suavet, C., Alexandre, A., Franchi, I.A., Gattacceca, J., Sonzogni, C., Greenwood, R.C., Folco, L., Rochette, P., 2010. Identification of the parent bodies of micrometeorites with high-precision oxygen isotope ratios. *Earth and Planetary Science Letters*. 293(3-4), 313-320.

- Suavet, C., Rochette, P., Kars, M., Gattacceca, J., Folco, L., Harvey, R.P., 2009. Statistical properties of the Transantarctic Mountains (TAM) micrometeorite collection. *Polar Science*. 3(2), 100-9.
- Suttle, M. D., Hasse, T., & Hecht, L., 2021. Evaluating urban micrometeorites as a research resource - A large population collected from a single rooftop. *Meteoritics & Planetary Science*. 56(8), 1531-1555.
- Swain, A.K., 2021. Status Note on Indian Attempts to Search for Meteorites in Antarctica. *Journal of the Geological Society of India*. 97(8), 915-922.
- Takayanagi, M., Ozima, M., 1987. Temporal variation of $^3\text{He}/^4\text{He}$ ratio recorded in deep-sea sediment cores. *Journal of Geophysical Research Solid Earth*. 92(B12), 12531-12538.
- Taylor, S., Matrajt, G., Guan, Y., 2012. Fine-grained precursors dominate the micrometeorite flux. *Meteoritics & Planetary Science*. 47(4), 550-564.
- Taylor, S., Delaney, J., Herzog, G., 2010. A CAI Micrometeorite. 41st LPSC. 1205.
- Taylor, S., Herzog, G.F., Delaney, J.S., 2007. Crumbs from the crust of Vesta: Achondritic cosmic spherules from the South Pole water well. *Meteoritics & Planetary Science*. 42(2), 223-33.
- Taylor, S., Lever, J. H., Harvey, R. P., 2000. Numbers, types, and compositions of an unbiased collection of cosmic spherules. *Meteoritics & Planetary Science*. 35(4), 651-666.
- Taylor, S., Lever, J. H., Harvey, R. P., 1998. Accretion rate of cosmic spherules measured at the South Pole. *Nature*. 392, 899–903.
- Toppani, A., Libourel, G., Engrand, C., Maurette, M., 2001. Experimental simulation of atmospheric entry of micrometeorites. *Meteorit. Planet. Sci.* 36, 1377-1396.
- Uścińowicz, G., 2012. Spherical, magnetic grains of extraterrestrial origin, isolated from Pacific sediments. *Oceanological and Hydrobiological Studies*. 41(3), 48-53.
- Van Ginneken, M., Genge, M. J., Folco, L., Harvey, R.P., 2016. The weathering of micrometeorites from the Transantarctic Mountains. *Geochim. Cosmochim. Acta*. 179, 1–31.
- Van Ginneken, M., Folco, L., Cordier, C., Rochette, P., 2012. Chondritic micrometeorites from the Transantarctic Mountains. *Meteoritics & Planetary Science*. 47(2), 228-247.
- Yada, T., Nakamura, T., Takaoka, N., Noguchi, T., Terada, K., Yano, H., Nakazawa, T., Kojima, H., 2004. The global accretion rate of extraterrestrial materials in the last glacial period estimated from the abundance of micrometeorites in Antarctic glacier ice. *Earth, planets and space*. 56(1), 67-79.
- Yiou, F., Raisbeck, G. M., Jéhanno, C. 1991. The micrometeorite flux to the Earth, during the last~ 200,000 years as deduced from cosmic spherule concentration in Antarctic ice cores. *Meteoritics*. 26, 412.

Figure Captions

Fig.1

Location map of the study area, Central Indian Ocean Basin (CIOB) where the cosmic spherules are recovered.

Fig. 2

Histogram plot of Numbers versus diameter of studied cosmic spherules. The peak diameter of the spherule is lying between 200 and 250 μm .

Fig. 3

Representative BSE images showing particles of various types of MMs in the current study. (a) Barred (b) Glass (c) Cryptocrystalline (d) Porphyritic (e) I Type (f) G Type (g) Scoriaceous (h) Relict Grain Bearing (i) Pyroxene bearing

Fig. 4

Percentage of various types of MMs used in the current study.

Fig. 5

Bulk major elemental ratio normalised with respect to Si and CI chondrite of various types of cosmic spherules. The red line denotes values for the CI chondrite.

Fig. 6

Representative BSE images showing various olivine morphologies found in studied cosmic spherules. (a) and (b) Cosmic spherules with skeletal olivines; (c) and (d) Cosmic spherules with cumulative olivines where there is an increment of grain size ; (e) and (f) Non-cumulative porphyritic olivine cosmic spherules with nearly even crystal distribution ; (g) Platy olivine cosmic spherules (h) Cosmic spherules with zoned olivine grains.

Fig. 7

Histogram showing forsterite content in analysed porphyritic and relict olivines.

Fig. 8

Comparison of major oxides in relict and porphyritic olivines with known olivine found in known meteorites. The data used for comparison is compiled from the literature (Kurat et al. 1989; Steele 1992; Bearley and Jones 1998; Jones and Carey 2006; Russel et al. 2010; Rudraswami et al. 2011; Rudraswami et al. 2016)

Fig. 9

Histogram plot of bulk Al/Si, Mg/Si, Fe/Si (normalized to CI values) of different S-type spherules. The value for CI, CV, CM, and CO, along with H, L, LL, EH, and EL, is shown by a dashed line.

Fig. 10

Fe-Mg-Mn systematics for glass spherules showing their chondritic origin.

Fig. 11

The plot of fayalite content (mole %) versus CaO (wt%) was measured in relict olivines from relict bearing and porphyritic spherules. The dashed lines show the compositional range of olivine in chondrules of type I and II and olivine in a matrix of carbonaceous chondrites (Beckerling and Bischoff, 1995). The bottom dash line is for olivines in ordinary chondrites.

Fig. 12

BSE images of cosmic spherules showing features formed due to alteration during atmospheric entry. (a) and (b) shows melt patch formed due to segregation of metallic and silicate phases; (c) and (d) shows dendritic magnetites formed during atmospheric entry; (e) and (f) Cosmic spherules with escaped metallic bead ; (g) and (h) Cosmic spherules with zoned olivines.

Fig. 13

Variation of various major oxides (FeO, MgO, SiO₂, MnO, CaO and Al₂O₃) across zoned olivines from core to rim.

Fig. 14

Variation of NiO (wt. %) in Relict and porphyritic olivines in the cosmic spherules.

Fig.15

Representative BSE images showing etching of cosmic spherules. (a)-(c) shows etched barred cosmic spherules with variable dissolution rims; (d)-(f) shows etching in porphyritic cosmic spherules. (g)-(h) shows selective dissolution of silicate phases in comparison to dendritic magnetites.

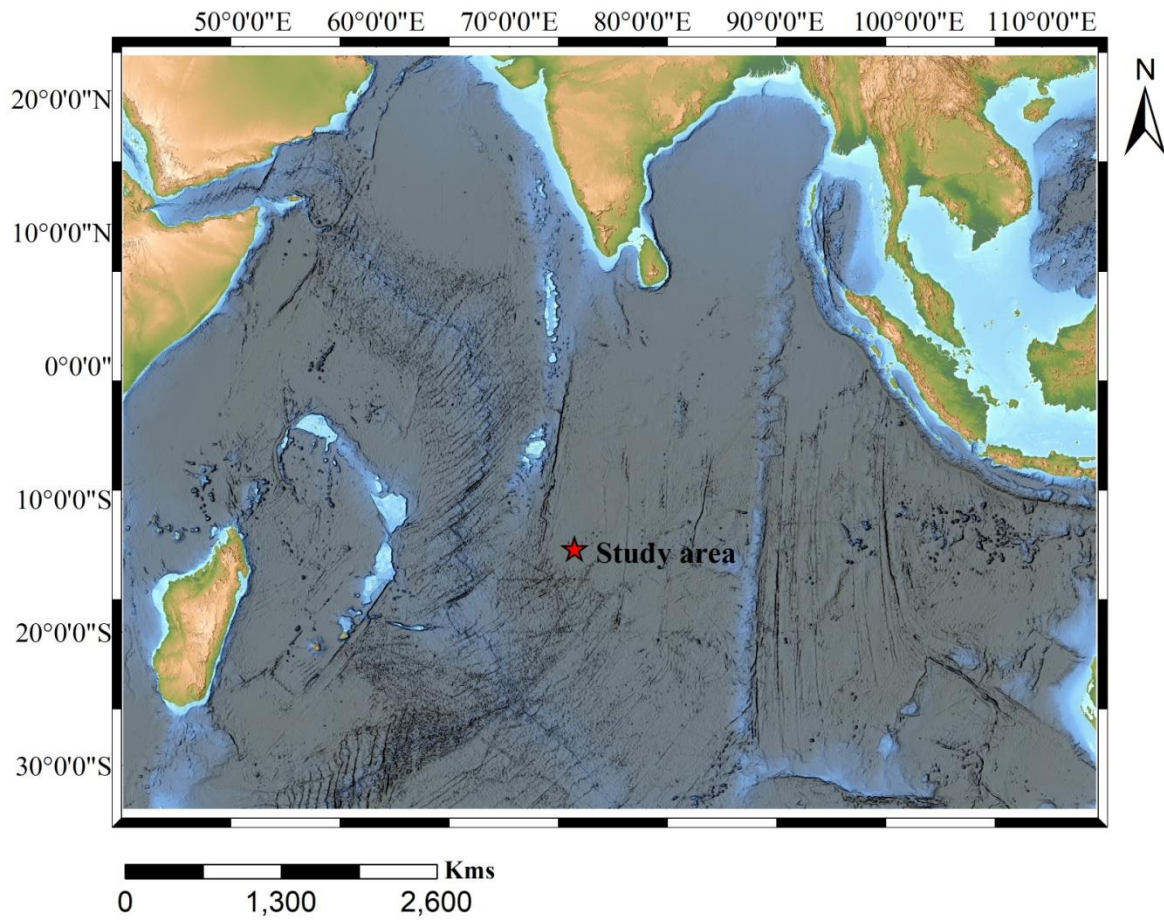


Fig.1 Location map of the study area, Central Indian Ocean Basin (CIOB) where the cosmic spherules are recovered.

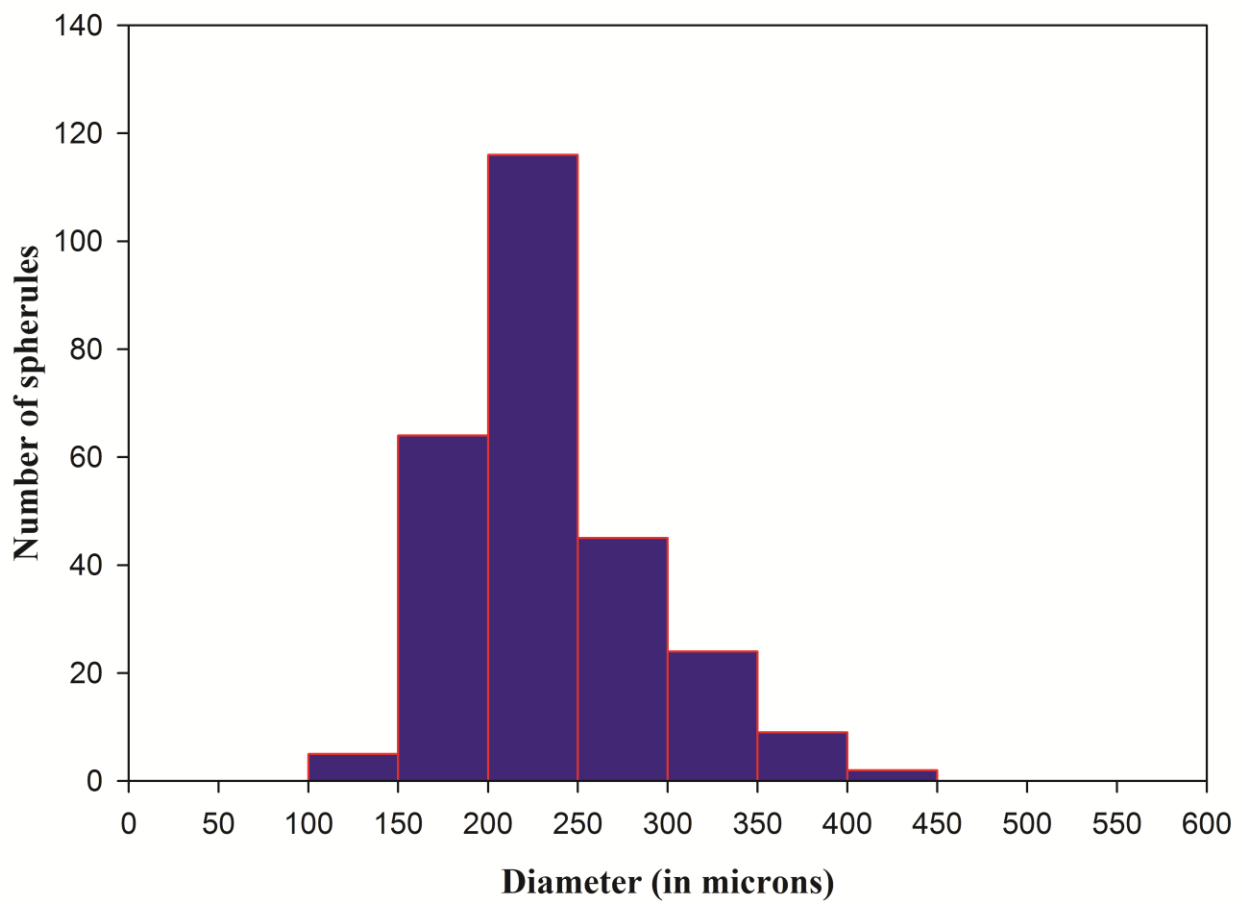


Fig.2 Histogram plot of Numbers versus diameter of studied cosmic spherules. The peak diameter of the spherule is lying between 200 and 250 μm .

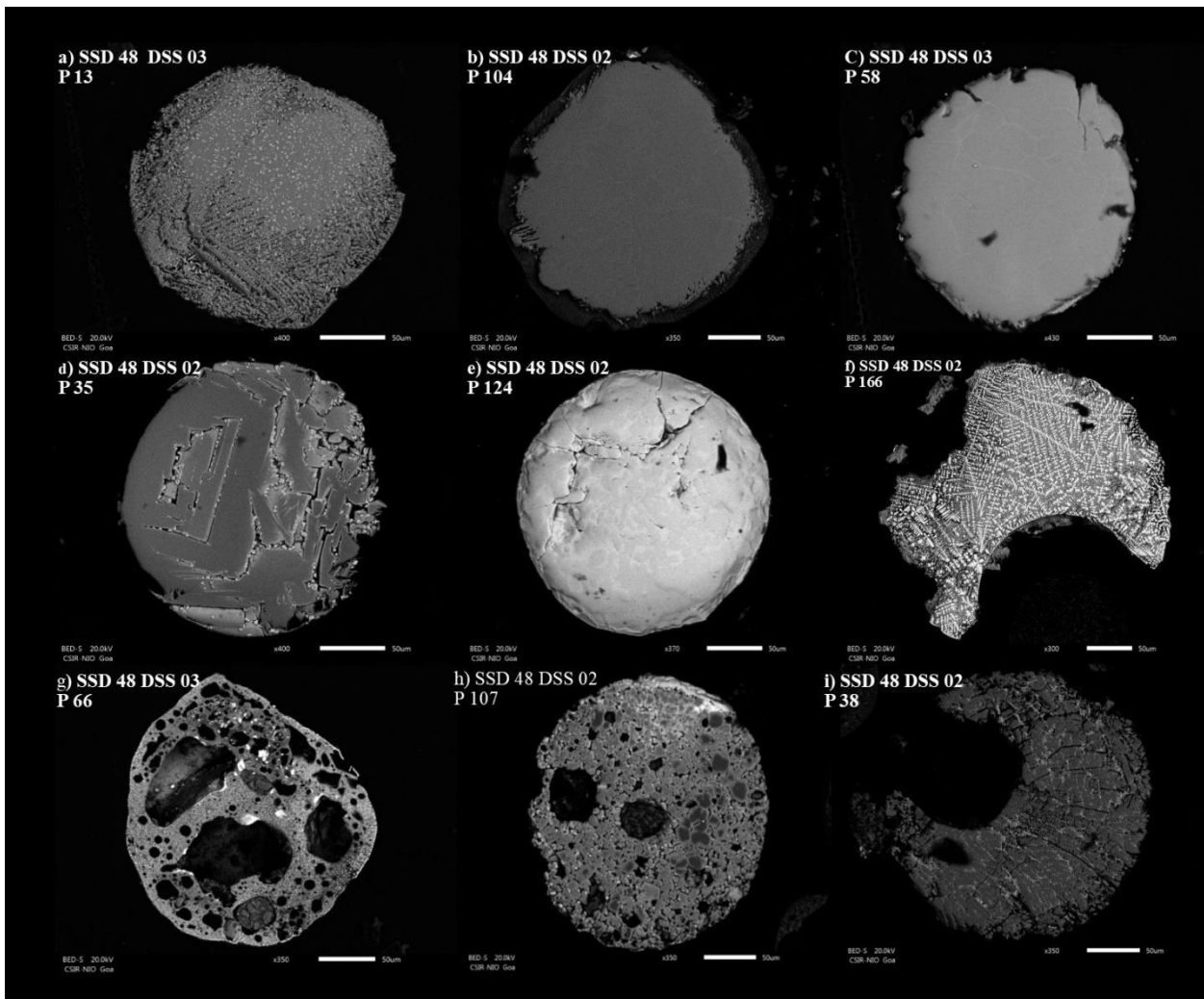


Fig. 3 Representative BSE images showing particles of various types of MMs in the current study. (a) Barred (b) Glass (c) Cryptocrystalline (d) Porphyritic (e) I Type (f) G Type (g) Scoriaceous (h) Relict Grain Bearing (i) Pyroxene bearing

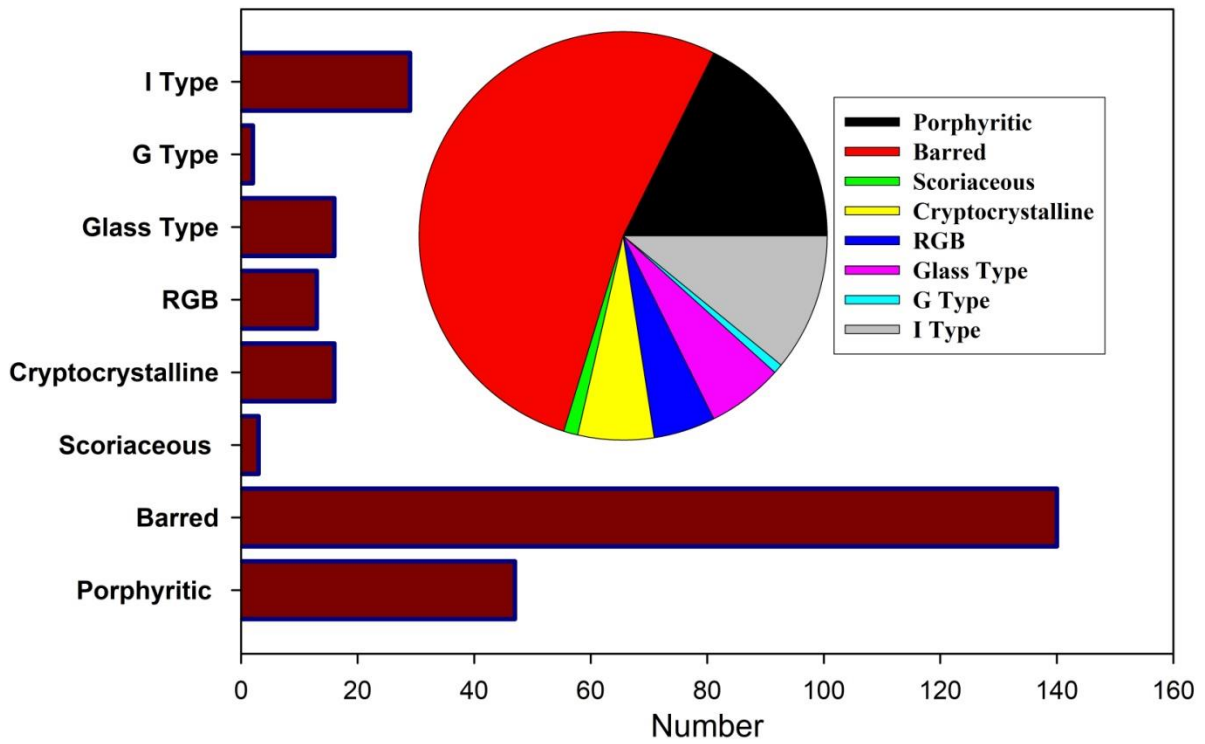


Fig.4 Percentage of various types of MMs used in the current study.

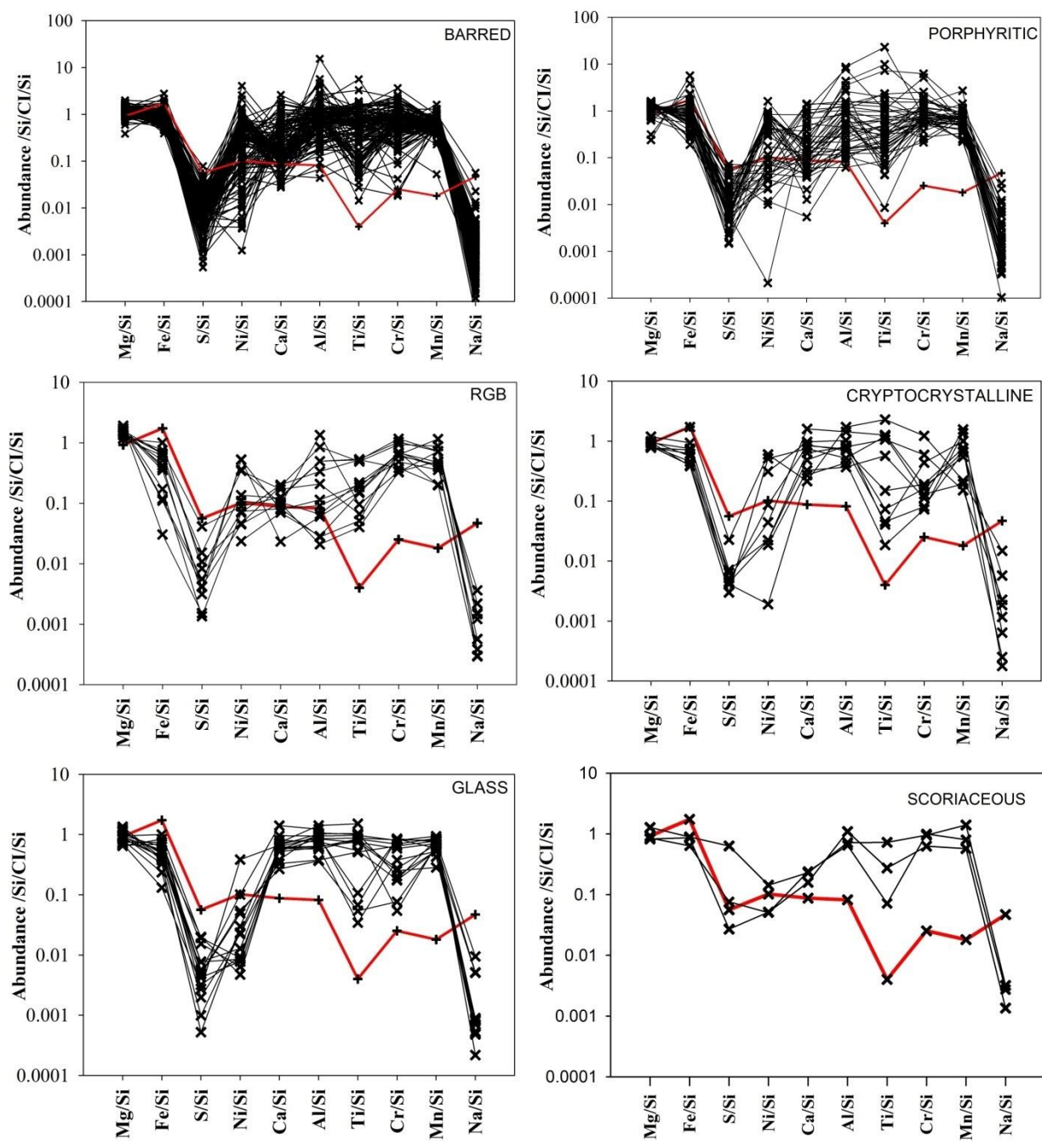


Fig.5 Bulk major elemental ratio normalised with respect to Si and CI chondrite of various types of cosmic spherules. The red line denotes values for the CI chondrite

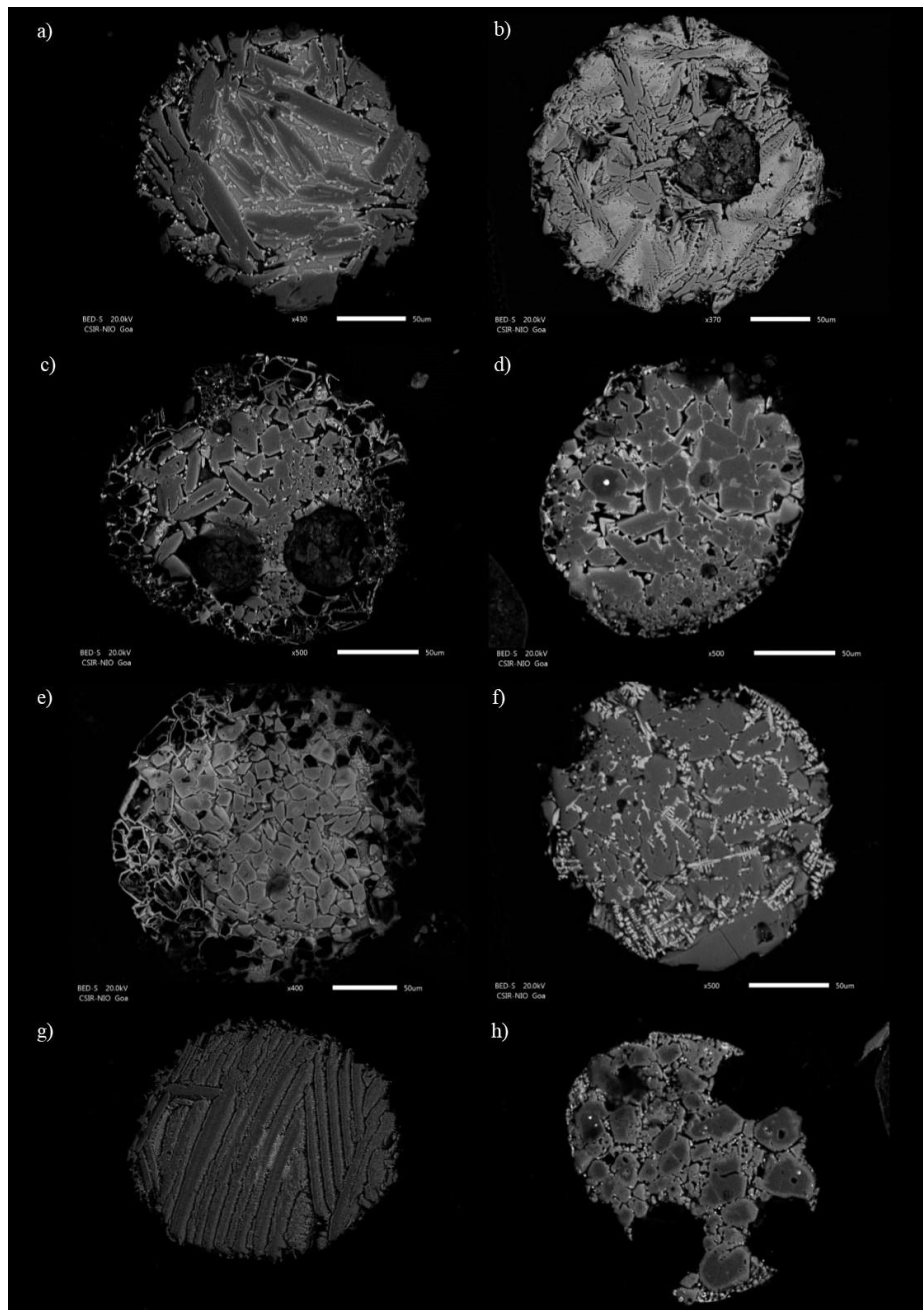


Fig.6 Representative BSE images showing various olivine morphologies found in studied cosmic spherules. (a) and (b) Cosmic spherules with skeletal olivines; (c) and (d) Cosmic spherules with cumulative olivines where there is an increment of grain size ; (e) and (f) Non-cumulative porphyritic olivine cosmic spherules with nearly even crystal distribution ; (g) Platy olivine cosmic spherules (h) Cosmic spherules with zoned olivine grains.

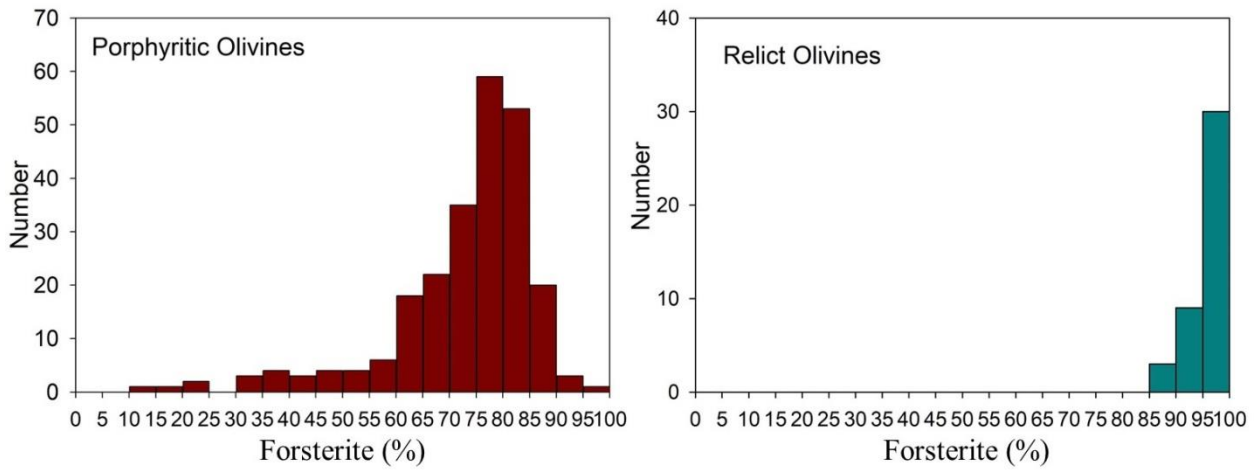


Fig.7 Histogram showing forsterite content in analysed porphyritic and relict olivines.

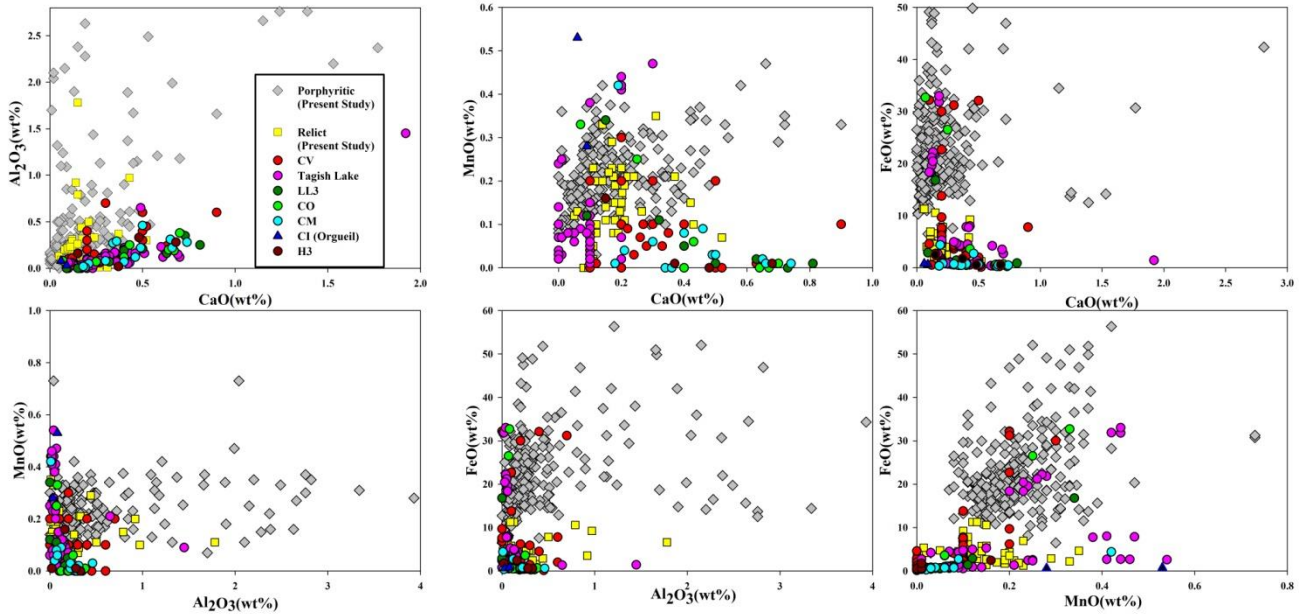


Fig. 8 Comparison of major oxides in relict and porphyritic olivines with known olivine found in known meteorites. The data used for comparison is compiled from the literature (Kurat et al. 1989; Steele 1992; Bearley and Jones 1998; Jones and Carey 2006; Russel et al. 2010; Rudraswami et al. 2011; Rudraswami et al. 2016)

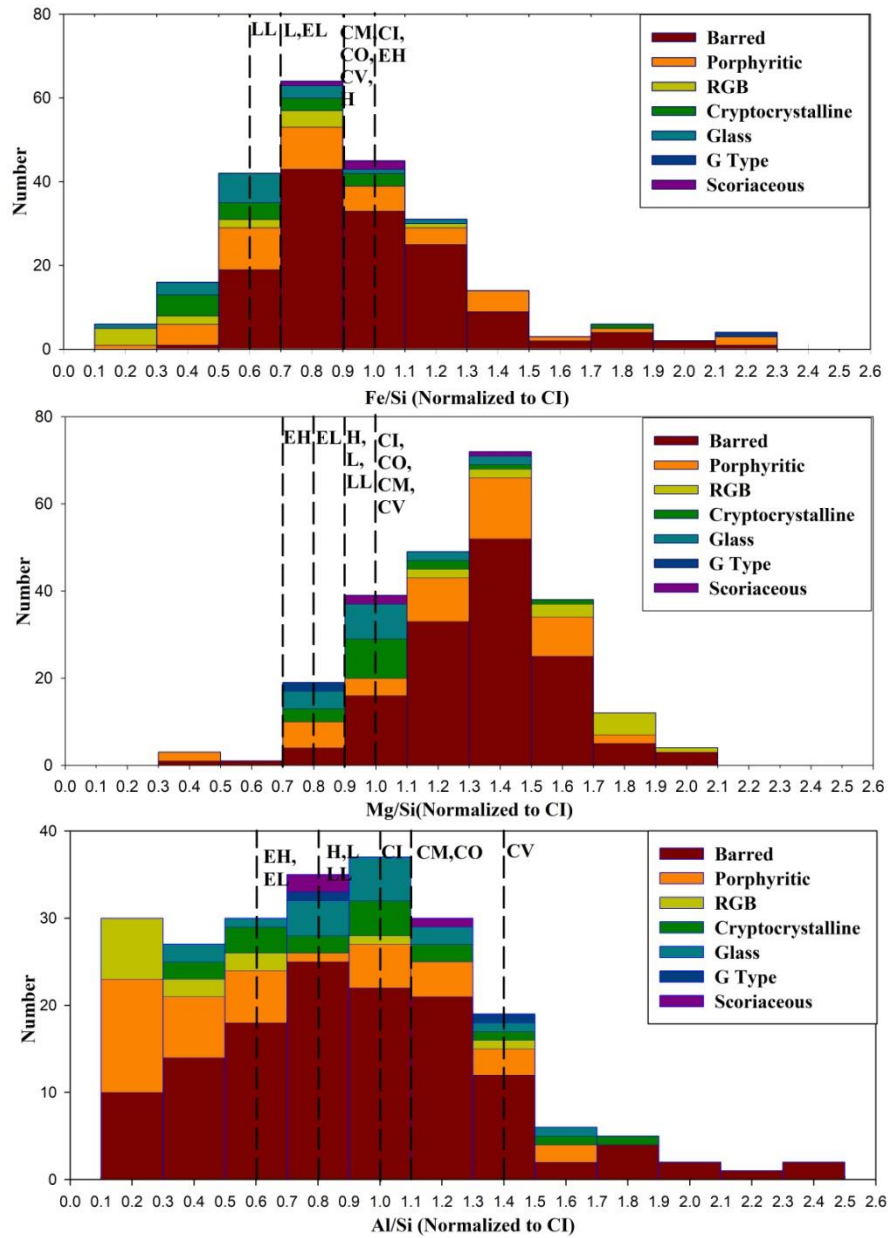


Fig.9 Histogram plot of bulk Al/Si, Mg/Si, Fe/Si(normalized to CI values) of different S-type spherules. The value for CI, CV, CM, and CO, along with H, L, LL, EH, and EL, is shown by a dashed line.

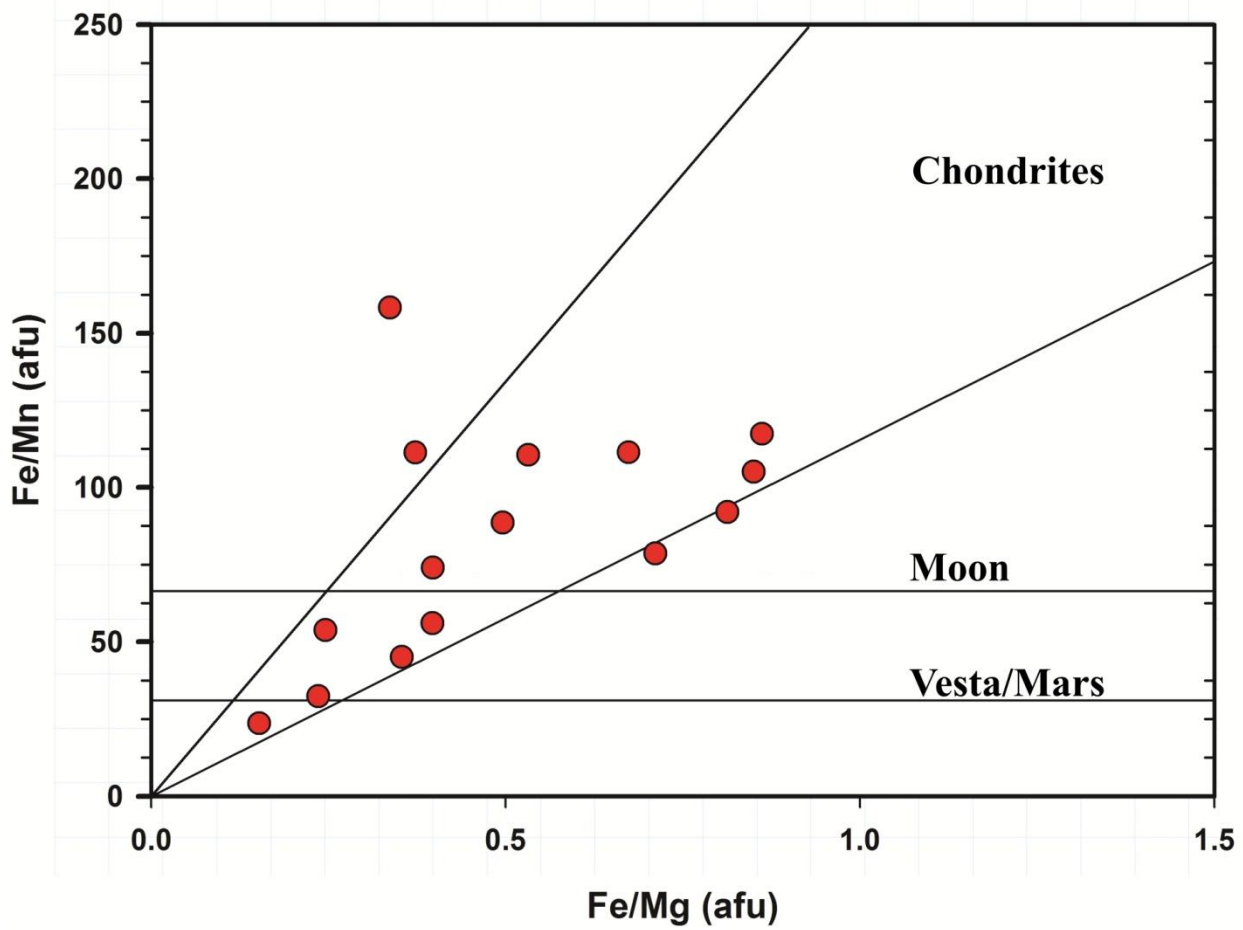


Fig. 10 Fe-Mg-Mn systematics for glass spherules showing their chondritic origin

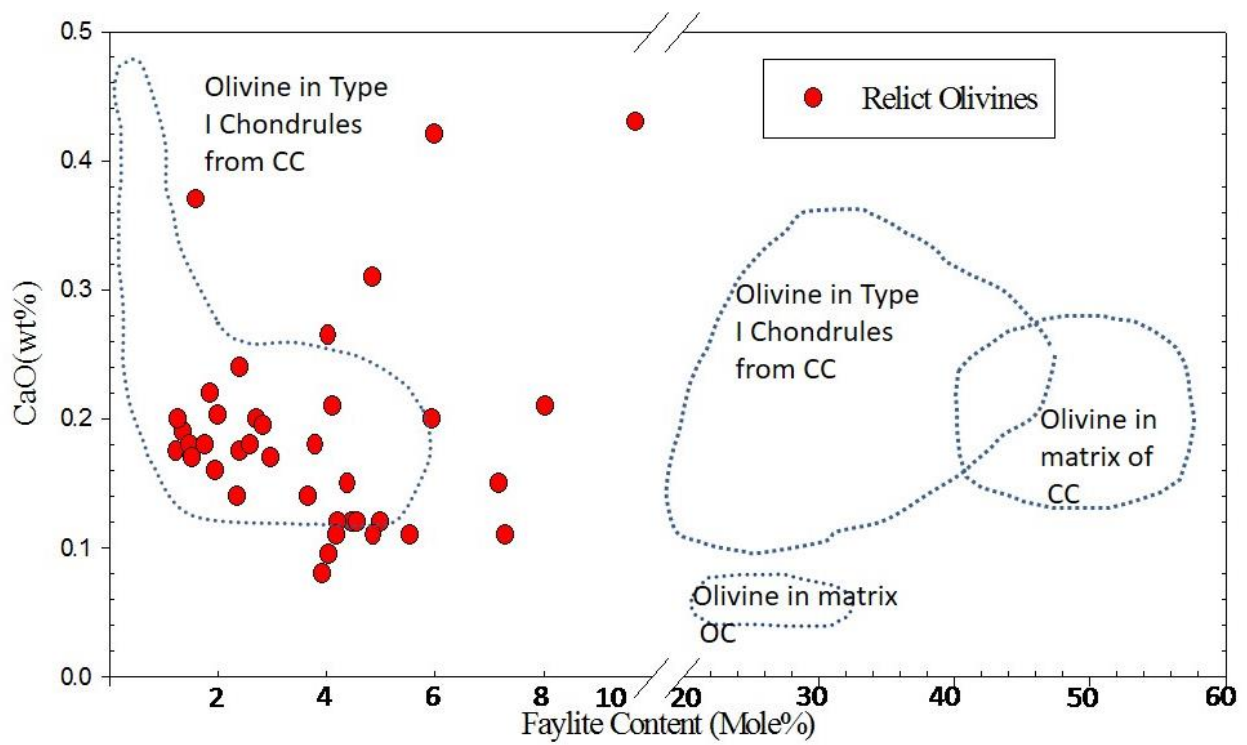


Fig. 11 The plot of fayalite content (mole%) versus CaO (wt%) was measured in relict olivines from relict bearing and porphyritic spherules. The dashed lines show the compositional range of olivine in chondrules of type I and II and olivine in a matrix of carbonaceous chondrites (Beckerling and Bischoff, 1995). The bottom dash line is for olivines in ordinary chondrites.

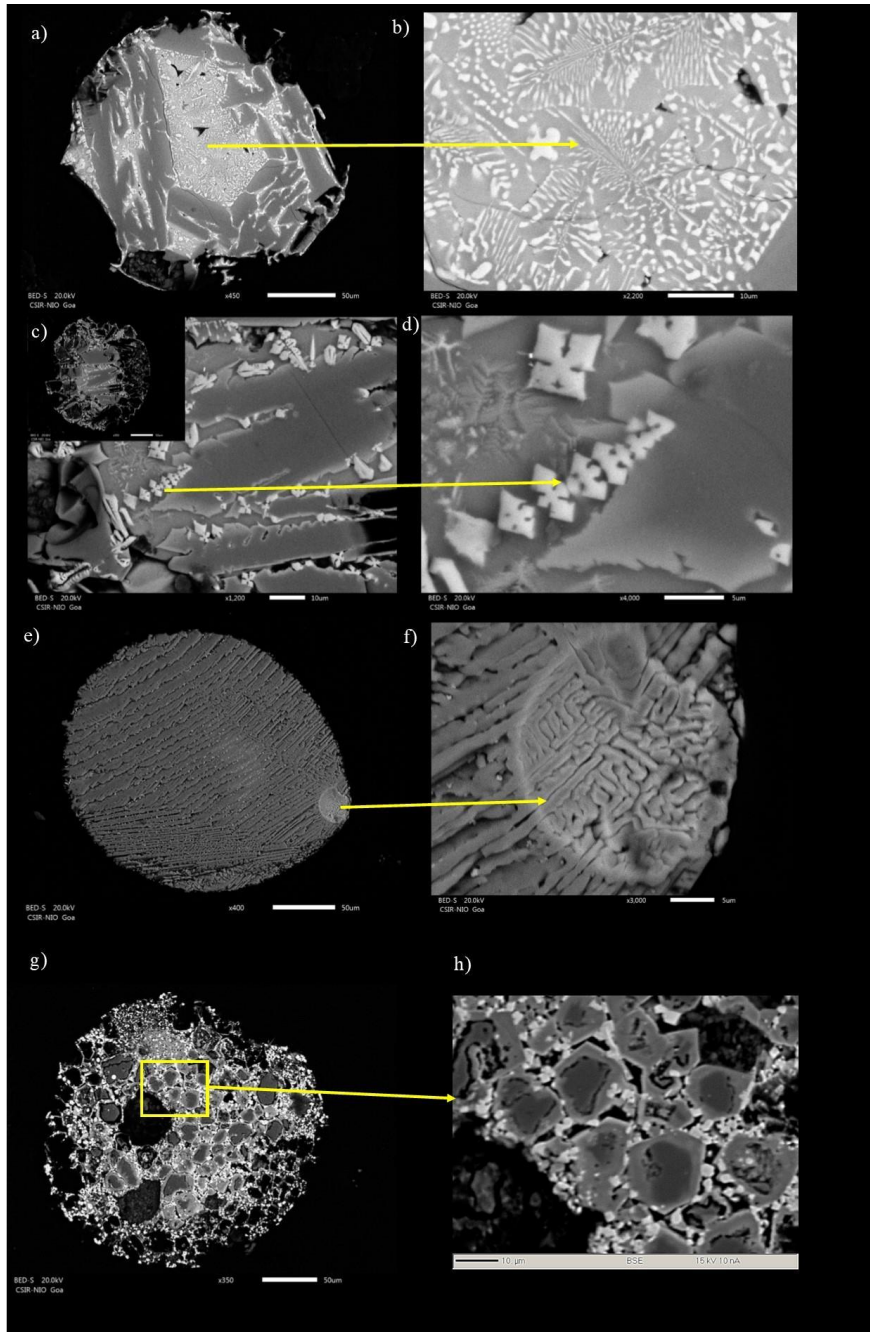


Fig.12 BSE images of cosmic spherules showing features formed due to alteration during atmospheric entry. (a) and (b) shows melt patch formed due to segregation of metallic and silicate phases; (c) and (d) shows dendritic magnetites formed during atmospheric entry; (e) and (f) Cosmic spherules with escaped metallic bead ; (g) and (h) Cosmic spherules with zoned olivines.

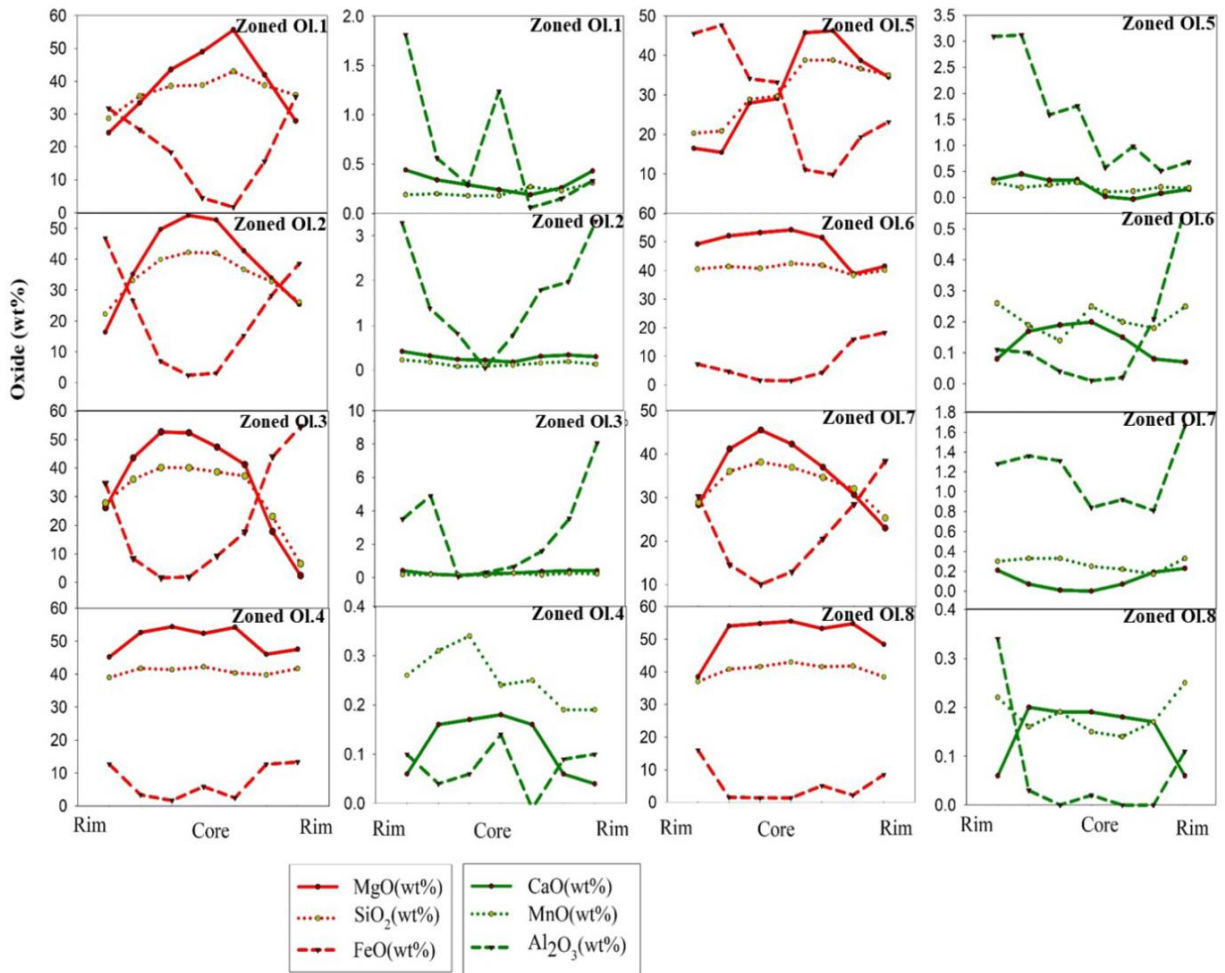


Fig. 13 Variation of various major oxides (FeO, MgO, SiO₂, MnO, CaO and Al₂O₃) across zoned olivines from core to rim.

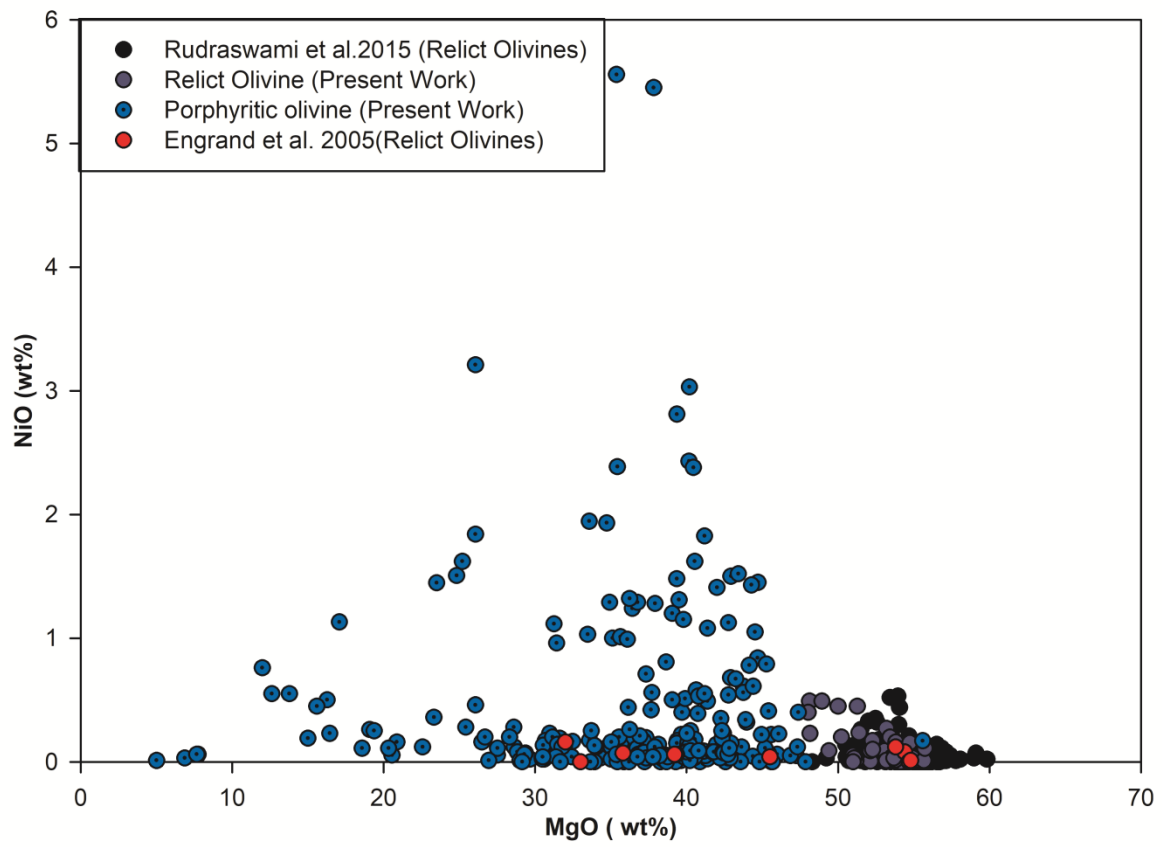


Fig. 14 Variation of NiO (wt. %) in Relict and porphyritic olivines in the cosmic spherules.

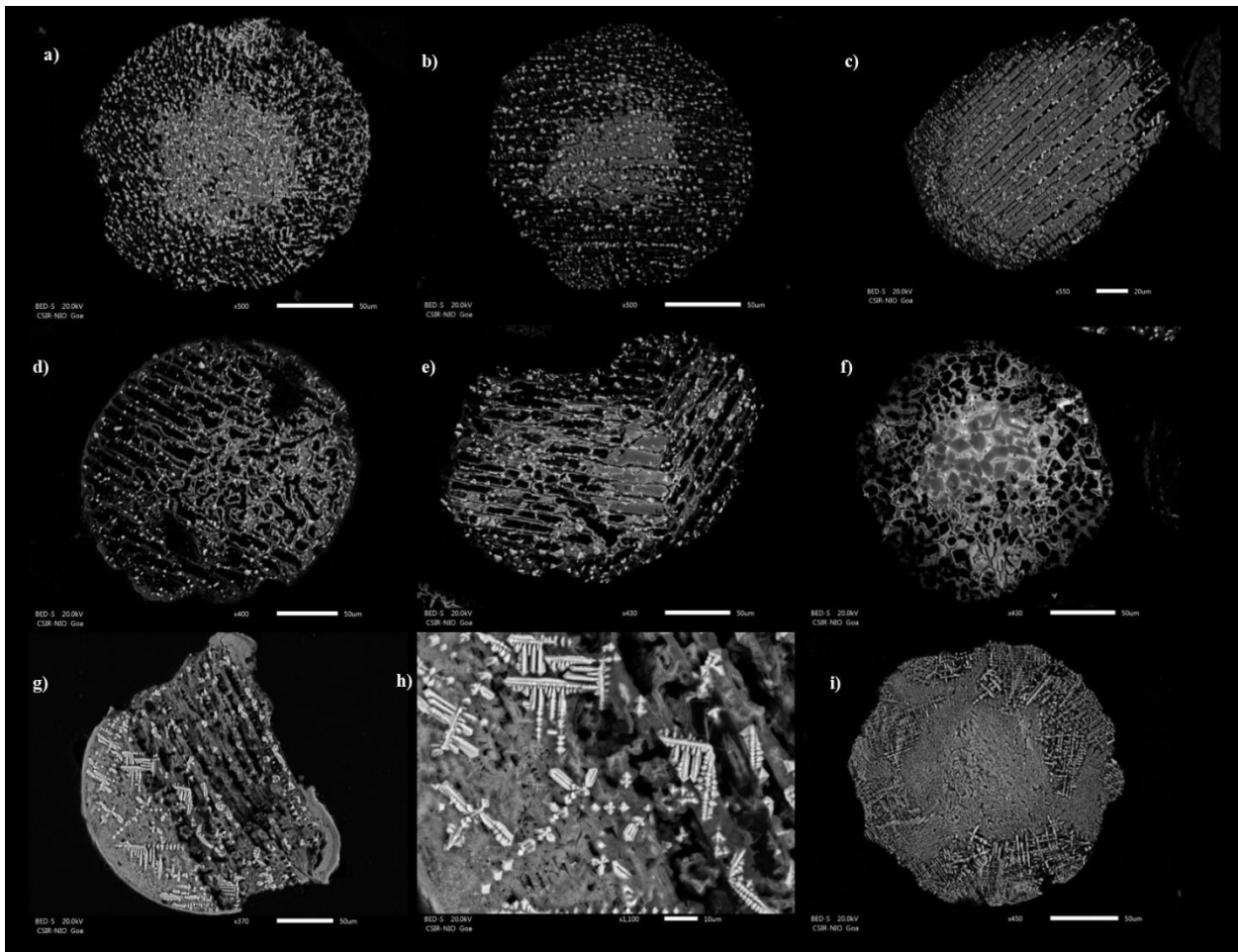


Fig.15 Representative BSE images showing etching of cosmic spherules. (a)-(c) shows etched barred cosmic spherules with variable dissolution rims; (d)-(f) shows etching in porphyritic cosmic spherules. (g)-(h) shows selective dissolution of silicate phases in comparison to dendritic magnetites.